EXPERIMENTAL INVESTIGATION ON QUENCHING OF LOW THERMAL CONDUCTIVE MATERIAL COATED CRYOGENIC TRANSFER LINE

A PROJECT REPORT

Submitted by

NITHYA KRISHNAN

TKM20MEIR11

to

APJ Abdul Kalam Technological University
in partial fulfilment of the requirements for the award of
Master of Technology in
Industrial Refrigeration and Cryogenic Engineering
(Mechanical Engineering)

Department of Mechanical Engineering

TKM College of Engineering, Kollam

September 2022

DEPARTMENT OF MECHANICAL ENGINEERING

TKM COLLEGE OF ENGINEERING, KOLLAM

CERTIFICATE

This is to certify that the report entitled '*Experimental Investigation on Quenching of Low Thermal Conductive Material Coated Cryogenic Transfer*' is the report presented by **NITHYA KRISHNAN, TKM20MEIR11** during **2021-2022** in partial fulfilment of the requirements for the awards of the Degree of Master Technology in Industrial Refrigeration And Cryogenic Engineering, (Mechanical Engineering) of APJ Abdul Kalam Technological University.

Guide:
Dr. Jesna Mohammed
Associate Professor
Dept. of Mechanical Engineering
TKM College of Engineering, Kollam

Coordinator:
Dr. Shafi K A
Professor
Dept. of Mechanical Engineering
TKM College of Engineering, Kollam

Dr. Dileep P N
Head of the Department
Dept. Mechanical Engineering
TKM College of Engineering, Kollam

DECLARATION

I, NITHYA KRISHNAN hereby declare that, this project report entitled **Experimental Investigation on Quenching of Low Thermal Conductive Material Coated Cryogenic Transfer Line** is the bonafide work of mine carried out under the supervision of Dr. Jesna Mohammed, Associate Professor, Dept. of Mechanical Engineering TKM College of Engineering, Kollam. I declare that, to the best of my knowledge, the work reported herein does not form part of any other project or dissertation on the basis of which a degree or award was conferred on an earlier occasion to any other candidate. The content of this report is not being presented by any other student to this or any other University for the award of a degree.

NITHYA KRISHNAN
University Register No: TKM20MEIR11 of year 2020-2022

Dr. Jesna Mohammed
Associate professor
Dept. of Mechanical Engineering
TKM College of Engineering, Kollam

Dr. Dileep P N
Head of the Department
Dept. Mechanical Engineering
TKM College of Engineering, Kollam

Date: 12/09/2022

ACKNOWLEDGEMENT

Any attempt at any level cannot be satisfactorily completed without the support and guidance of learned people. I owe to great many people whose constant support and motivation that has encouraged me to come up with this project. I would like to express my heartfelt thanks to **Dr. Jesna Mohammed**, Associate Professor, Department of Mechanical Engineering, TKM College of Engineering for being instrumental in the completion of my project with his guidance.

I express my deep sense of gratitude to **Dr. Dileep P N**, Professor and Head of Department, TKM College of Engineering from bottom of heart for lending me all facilities and support for completion of this project. I thank, **Dr. Shafi K A**, P G Coordinator, Department of Mechanical Engineering, TKM College of Engineering for giving their constant support for doing this project. I would like to thank **Dr. Mohammed Sajid N K**, Professor (Rtd.) and former Head of Department, Department of Mechanical Engineering, TKM College of Engineering for lending me all the facilities and support.

I thank **Dr. Krishna Kumar T S**, Associate Professor, Department of Mechanical Engineering for his constant support regarding the proceedings of the project. I would like to thank **Prof. Saibi,** Assistant Professor and Head of chemical Department and **Dr. Femina A**, Professor, Department of Chemical Engineering. I would like to thank Director and other staffs of **KMML** for their constant support regarding the proceedings of the project. I also extend my regards to instructors: **Mr Y Johnson**, **Subin Basheer**, and tradesmen: **Mr Nazeer Khan A**, **Afsal S** Department of Mechanical Engineering for their constant support during the proceedings of my project and I thank **Mr Vyshakh V**, Junior Research Fellow, Department of Mechanical Engineering and **Rahul Rajeev**, **Gokul Hareesh**, **Abhijith K R** M-tech students Department of Mechanical Engineering other college staffs for the technical and nontechnical assistance given for the project.

NITHYA KRISHNAN

Place: Kollam

Date: 12/09/2022

ABSTRACT

Cryogenic fluids is frequently encountered in many applications, such as cryogenic cooling, material processing, biological tissue preservation, food engineering, aerospace field, cooling of superconducting devices and chemical process etc. It has been understood in pool quenching experiments, that the thin low thermal conductive coating layer on the wall can greatly improve the cooling performance, while less is known about flow quenching. In the present study, the experiments are to investigate cryogenic flow quenching of the horizontal stainless steel tubes with different coating layers on the inner walls. Two types of coating layers with various thickness were prepared with the help of paint epoxy on the inner surface of the tube. To investigate the thermo-electric property and thickness of the coating layer on the quenching performance, as compared with the uncoated and epoxy coated tube. Here we are using magnetic stirring and sonication method for coating. It is shown that a thin coating layer on the inner tube wall can significantly shorten the quenching time and enhance the heat transfer performance. To analyse the heat transfer characteristics, an inverse heat conduction equation with consideration of variable thermo-physical properties and thermal contact resistance was numerically solved to obtain the inner wall temperature and heat flux. The reason for the quenching enhancement can be attributed to the shortening of film boiling regime of cryogenic quenching in the inner surface by coating layer which allows the improvement of Leidenfrost point (LPF) temperature.

Keywords: Cryogenic quenching, Liquid Nitrogen, Flow boiling, coating layer

CONTENTS

LIST OF FIGURES

LIST OF TABLES

ABBREVATIONS

CHF	Critical Heat Flux
DAQ	Data Acquisition System
HTC	Heat Transfer Coefficient
LFP	Leiden Frost Point
LN_2	Liquid Nitrogen
MHF	Minimum Heat Flux Point
NPs	Nanoparticles
PTFE	Polytetrafluoroethylene
YSZ	Yttria-stabilized zirconia

CHAPTER 1

INTRODUCTION

Energy sectors typically use cryogenic liquids as coolants or fuels, including liquefied natural gas (LNG), liquid oxygen (LOX), liquid nitrogen (LN2), liquid hydrogen (LH2), and liquid helium (LHe). Due to their high specific impulse and ecologically favourable characteristics, cryogenic fluids are used as essential propellants for space launch vehicles. For carrying out cryogenic missions and building a properly functioning cryogenic system, the procedure of transporting cryogenic liquid through pipe line is essential. In most cases, the transfer line from a room is initially precooled to the necessary cryogenic temperature using a portion of transferring liquids as the coolant. The line chill-down time and the amount of cryogenic propellant used during this procedure must be kept to a minimum. It is essential to comprehend the transient heat transfer mechanism of the operation in order to control the cryogenic line chill-down procedure and reduce the consumption of cryogenic liquid. Instabilities in pressure and fluid velocity, as well as exceptionally huge temperature variations between the pipe wall and the cryogenic fluid, all contribute to the intricate physical phenomena that occur during the chill-down of cryogenic lines.

Quenching is a transient heat and mass transfer phenomenon when a solid surface at a high temperature is cooled by a liquid whose boiling temperature is lower than solid surface temperature. Nowadays, due to the increasing use of cryogenic fluids, cryogenic quenching is frequently encountered in many fields, such as aerospace, cryosurgery and superconducting magnet cooling, etc.

There are several heat transfer stages in a cryogenic quenching, during which the heat transferring to the liquid can only come internally from the thermal capacity (internal energy) of the cryo-genically quenched object.

1.1 NATURE OF BOILING PROCESS

When the temperature of the liquid is lower than the saturation temperature, the liquid is called undercooled. If the temperature is above the saturation level it is called superheated liquid. Vapor can form only from superheated or saturated liquid.

Boiling can be classified as pool boiling and flow boiling. Boiling in the case of the fire tube of shell boiler will come under this category. Boiling as during the flow of water and steam (two phase fluid) through a tube in water tube boilers with wall heat flux is called flow boiling.

1.1.1 REGIMES OF BOILING

The physical phenomenon of pool boiling can be divided basically into four different regimes based on the excess temperature. The regimes are:

- **Purely Convective Region:** In thermodynamics, the requirement for boiling of pure substances to occur is that Twall = Tsat. In contrast, boiling doesn't happen in actual tests until the liquid is heated a few degrees above the saturation point. In order to support vapour production, the surface temperature must be a little bit higher than the saturation temperature. While the water surface will be covered in vapour in this boiling phase, bubbles are typically not visible..

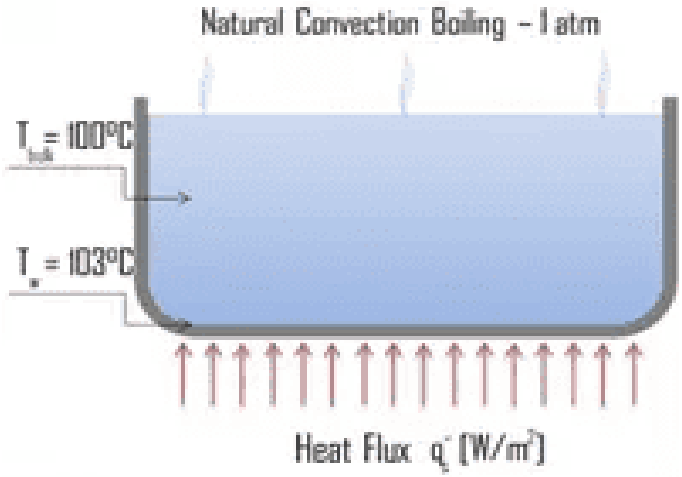

Fig.1.1 Natural Convection Boiling (Gaurav et al. 2019)

- **Nucleate Boiling:** The most common type of local boiling encountered in nuclear facilities is nucleate boiling. In nucleate boiling, steam bubbles develop at the heat transfer surface, separate, and then float into the fluid's main body. Because the heat produced at the surface is transferred directly into the fluid stream, such movement improves heat transmission. Because the bulk fluid temperature is lower than the heat transfer surface temperature where the bubbles were generated, once in the main fluid stream, the bubbles

burst. Because the energy generated at the heat transfer surface is "taken" away fast and effectively, this heat transfer technique is occasionally preferred.

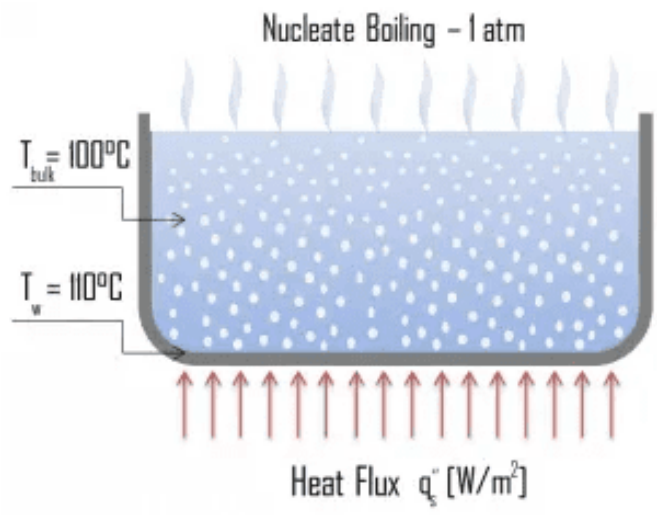

Fig.1.2 Nucleate Boiling (Gaurav et al. 2019)

- **Transition Boiling:** The nucleate boiling heat flux cannot be increased indefinitely. We call it the “critical heat flux” (CHF) at some value. The steam generated has the potential to create an insulating layer on the surface, which would reduce the heat transfer coefficient. This is owing to the fact that a sizable portion of the surface is covered by a vapour coating, which serves as thermal insulation because vapour has a lower thermal conductivity than liquid does. As soon as the critical heat flux is reached, transition boiling happens because boiling becomes unstable. The "boiling crisis" refers to the change from nucleate boiling to film boiling. Beyond the CHF limit, the heat transfer coefficient drops, and film boiling often ensues.

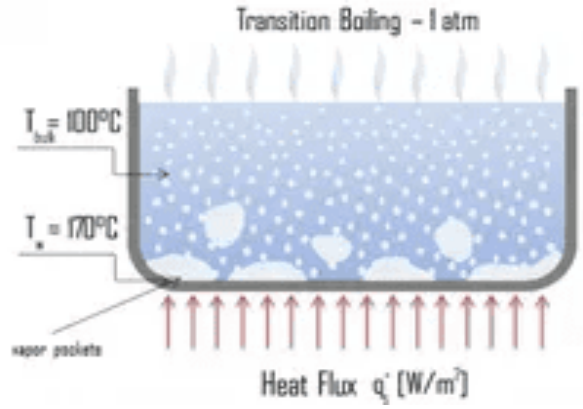

Fig. 1.3 Transition Boiling (Gaurav et al. 2019)

- **Film Boiling**: As the heat flow rises higher, a vapour film will cover the surface. Due to the vapour layer's greatly reduced capacity for heat transmission, this significantly lowers the convection coefficient. The surplus temperature rises to a very high value as a result. Beyond the Leidenfrost point, the surface is covered in a constant vapour sheet and the liquid phase is not in touch with it. Both conduction and radiation are used in this instance to deliver heat to the vapour. The apparatus will malfunction if the material can't endure this temperature without being damaged. The term "burnout" also applies to this issue. The absence of a deviation from nucleate boiling (DNB) during steady-state operation, typical operational transients, and predicted operational events is one of the most essential safety criteria for pressurised water reactors (AOOs).

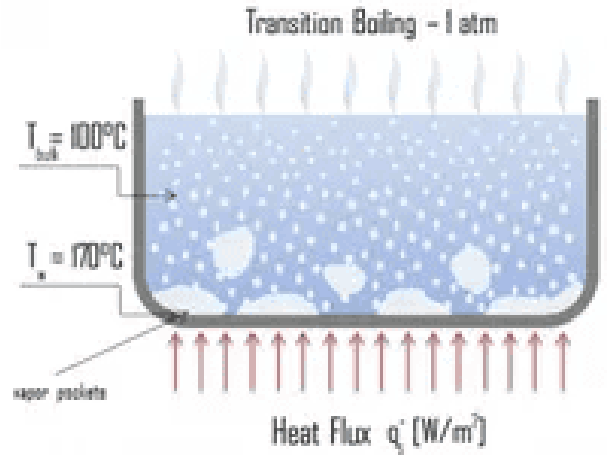

Fig. 1.4 Film Boiling (Gaurav et al. 2019)

1.2 FLOW BOILING

Flow boiling is nothing but forced convection boiling where the fluid is moved by an external device. The regimes of boiling and the heat flux curve are similar to the ones in pool boiling. The process occurs in modern high pressure forced circulation boilers. As sub-cooled liquid enters a heated tube with wall heat flux, initially heat transfer occurs by forced convection and the liquid is heated to saturation condition. After this condition, the flow is considered as two phase flow. The next regime is where bubbles form at the surface and then flow into the core where these may condense. At a later section the flow becomes slug type of flow alternately liquid and vapor filling the tube. This is followed by what is termed as annular flow with liquid flowing near the surface and vapor forming

the core. The heat flux reaches the maximum or critical value in this regime. The flow becomes unstable with the liquid film breaking out. The heat flux cannot be sustained without the material becoming overheated. Then the flow becomes what is called mist flow with small droplets of liquid floating in the vapor. The heat flux at this regime may be even lower than that in the forced convection regime. At this condition the radiation heat transfer coefficient will start increase.

1.2.1 TWO PHASE FLOW

Two-phase flow refers to any time that there are two-phases of substances traveling together in the same space. There are three basic phases of matter, solid, liquid, and gas. Liquids and gasses are traditionally labelled as fluids because they may be deformed without external force provided enough time elapses. Solids are not traditionally referred to as a fluid, but when presented as particles and the other fluid velocity is high enough, the solid then acts like a fluid. Two- phase flow presents itself as any combination of the four possible fluid phases. For many cases, the analysis of two-phase flow can be extended into multi-phase flows.

The flow does not have to consist of two-phases of the same substance. A perfect example of this is in coal furnaces where coal dust and air travel together as a particulate gas two-phase flow to the firing area of the furnace. When referring to cryogenic flow, however, it most often means that the two-phases are of the same substance.

Occasionally liquid-solid flow can be seen from the slight freezing of the fluid, but the primary two-phase flow seen in cryogens is liquid-gas. For the remainder of this thesis the phase “two-phase flow” refers to liquid-gas flows unless stated otherwise.

Liquid-gas two-phase flow occurs under a number of different conditions. In cryogenics, it is typically seen from two main causes. It can occur temporarily due to heat leak in the channel or it can occur due to the pressure dropping below the single-phase boundary. That being said, it is important to understand the relationship between three critical thermodynamic variables: temperature, pressure, and volume. Figure 1.5 shows the pressure vs. temperature and pressure vs. volume phase diagrams for pure substances,

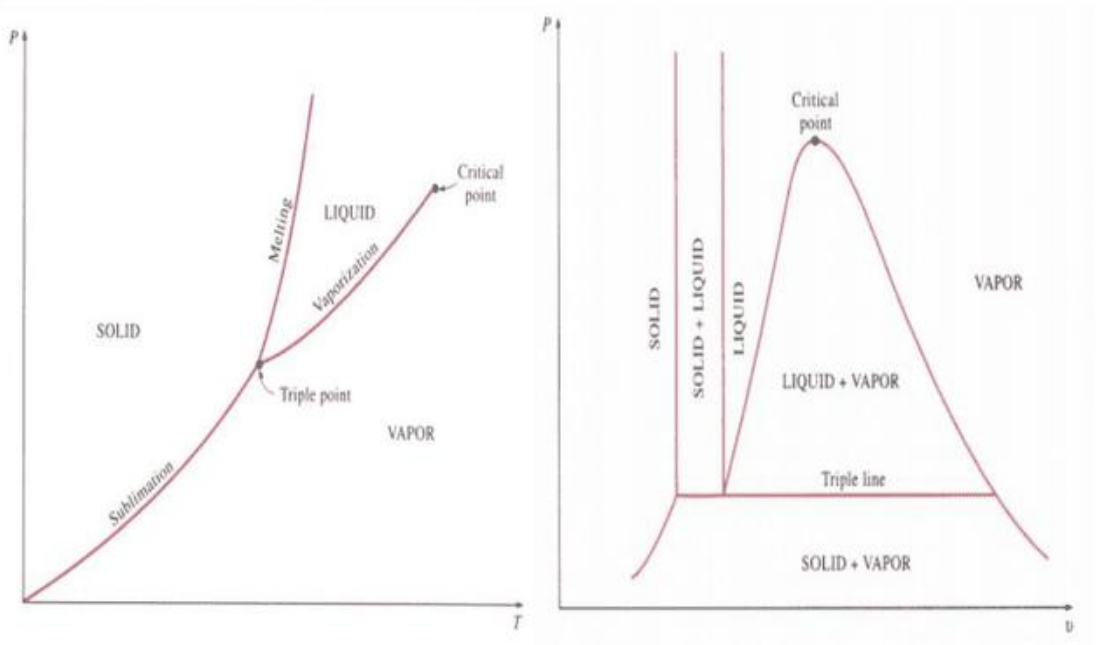

Fig. 1.5 Pressure vs. temperature diagram (left) and pressure vs. volume diagram (right) formost pure substances (Cengel et. al1997)

While liquid-gas two-phase flow is complicated, the flow patterns are distinct and can be consistently categorized. The interaction between the liquid and vapor phases is what primarily governs the behaviour of the flow and it varies as the velocities of the two-phases vary. Fluid characteristics like surface tension and viscosity are a large part of determining the flow behaviour. The flow behaves differently depending on if the channel is horizontal, vertical, or at an angle and low-gravity conditions cause the behaviour to change.

Figure 1.21 shows seven common flow patterns seen in horizontal two-phase flow. Some sources vary on the descriptions of the flow and the exact number of variations. This is because certain flow patterns are either very similar or are transitional regimes, so they are grouped together as a one pattern. While the flow regime cannot be determined from the void fraction or flow quality alone, the flow does typically change with respect to the increase or decrease of either of these values.

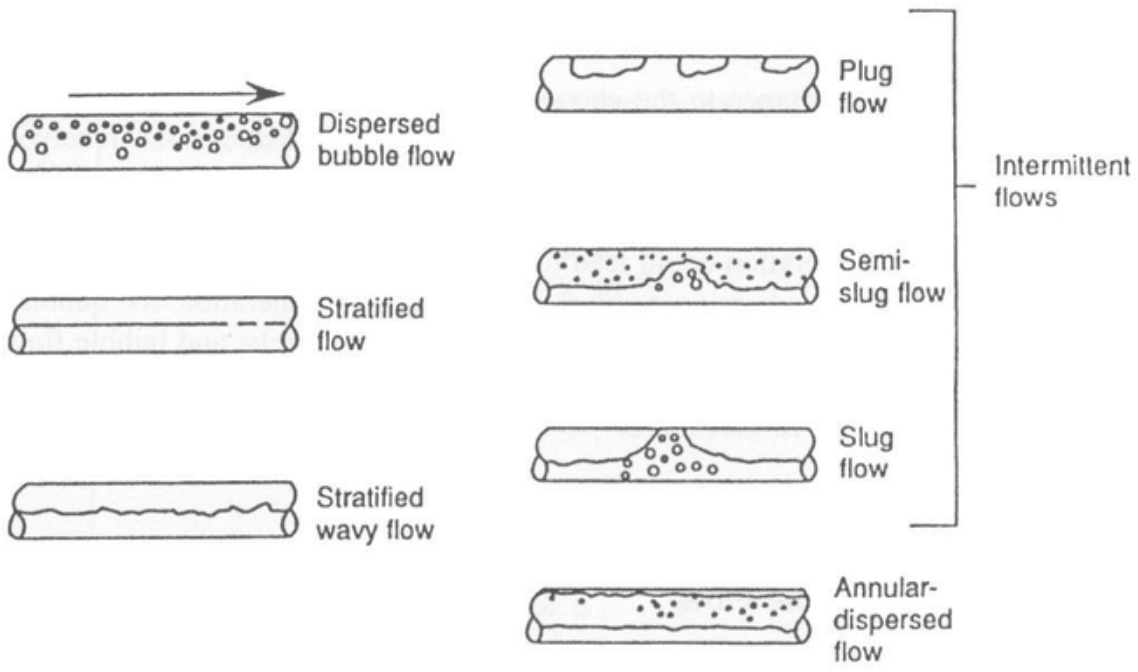

Fig. 1.6 The seven basic flow regimes for horizontal two-phase flow

(Levy et. al 1990)

A brief description of the flow patterns is given, arranged with respect to increasing flow quality

- **Bubble flow:** gas bubbles of various sizes flow at approximately the same velocity as the liquid. At lower liquid flow rate, the bubbles tend to travel at the top of the channel. At higher liquid flow rates, the bubbles are seen more evenly dispersed in the channel.
- **Plug flow:** as the gas flow rate increases, the small bubbles begin to combine to form ‘plugs’ of gas in the channel.
- **Stratified flow:** gravitational forces separate the liquid and gas phases. The liquid- gas interface is smooth. This is the rarest type of two-phase flow because it occurs most often in larger diameter pipes and laminar flow.
- **Wavy flow:** increasing mass flow rates creates disturbances at the phase boundary. The amplitude of these waves increases as the mass flow rates continue to increase. At the higher gas flow rates, semi-slug flow begins to appear and is sometimes considered a separate flow regime.

- **Slug flow:** wave amplitude is high enough that the liquid touches the top of the channel. The vapor is completely separated by ‘slugs’ of liquid traveling in the channel.
- **Annular flow:** At very high vapor flow rates, the liquid is forced to the walls of the channel and the gas travels in the center. At higher gas flow rates, liquid droplets are found in the vapor flow.
- **Dispersed flow:** The vapor flow rate is so much higher than the liquid flow rate that the liquid is broken into small droplets and carried in the vapor stream. As the vapor flow rate continues to increase, the droplets continue to get smaller and eventually become froth flow.

Two-phase flow regimes are often referred to as homogeneous or separated. Homogeneous flow consists of relatively even distribution of the liquid and gas phases across the cross section of the channel. Bubble flow, dispersed flow, and froth flow can all be considered homogeneous regimes. Separated flows are the regimes where the liquid and gas phases are separated. This often refers to flows that are in a stable state and are not time dependent, like stratified or annular flow regimes. Any of the flow regimes that vary with time are called intermittent flows. These include slug flow, semi-slug flow, and plug flow. As it was mentioned, gravity and orientation have an effect on the flow characteristics. When the channel is oriented vertically and the flow is traveling upwards, the effects of gravity allow for only five flow regimes: bubble, slug/plug, churn, annular, and dispersed flows. Churn flow is a highly turbulent regime between slug and annular flow. In this flow, the liquid near the tube walls continually pulses up and down due to gravity pulling the liquid down. In microgravity flows, we see dispersed bubble, bubble, slug, and annular flows. Microgravity flows are typically centred in the channels and tend to be less turbulent in their transitions between regimes thanks to the absence of gravity acting on two-phase.

1.3 PROBLEM FORMULATION

This study is to evaluate the performance of metal tubes with inner wall coatings of different low thermal conducting material during quenching heat transfer.

Cryogenic fluids is frequently used in such fields of cryogenic cooling, food engineering and chemical process, etc. in the present study, the experiments are conducted to investigate cryogenic flow quenching of the horizontal stainless steel tubes coated with

epoxy, Teflon and YSZ(Yttrium stabilized zirconium) coating layers on the inner walls. It shown that the thin coating layer on the inner tube wall can significantly shorten the quenching time and reduce the consumption of liquid nitrogen.

1.4 **THESIS OUTLINE**

- Chapter 1 Introduces the project topic and background.
- Chapter 2 Reviews recent development of cryogenic quenching.
- Chapter 3 Gives brief introduction about cryogenic quenching.
- Chapter 4 Presents the proposed experimental investigations.
- Chapter 5 Presents the experimental results.
- Chapter 6 Summaries of findings of the work.

CHAPTER 2

LITERATURE REVIEW

Cryogenic quenching happens often in situations where the safe functioning of equipment, the transportation, and storage of cryogenic fluids are crucial to the cooling process. A pre-cooling procedure is often required before normal operation since the starting temperature of the machinery or pipes is always significantly greater than the saturation temperature of the cryogenic fluid. The system is cooled down to a low temperature that is several hundred kelvins lower than the ambient temperature as a result of the quenching process, which is often inevitable and frequent.

2.1 STUDIES ON CRYOGENIC CHILLDOWN

Reid Shaeffer et al. (2013) conduct "an experimental study on liquid nitrogen pipe chill down and heat transfer with pulse flow" Upward flows in a circular tube with Reynolds numbers ranging from 2500 to 7000 were studied using liquid N2 as the working fluid. To determine the impact of flow oscillation, a comparison of continuous flow and pulse flow patterns on heat properties was given. Different square wave pulse flow techniques were looked at in order to better understand how flow pulsation affects the chilldown process. Continuous flow is more efficient for the majority of boiling regimes at low Reynolds numbers, whereas pulse flow is most effective for the film boiling regime at higher Reynolds numbers. Continuous flows with high Reynolds numbers are often more effective in transferring heat than other patterns or those with lower Reynolds numbers in terms of overall efficiency. The fastest chilldown times are constantly provided by continuous flow.

Lingxue Jin et al. (2016) describes the cryogenic chill-down experiments that are conducted on a 12.7mm outer diameter, 1.25mm wall thickness and 7m long stainless steel horizontal pipe with liquid nitrogen (LN_2). In order to reduce heat loss from ambient temperature and make it simple to numerically model the operation, the pipe is vacuum insulated throughout the experiment. At a site 5.5m away from the pipe inlet, the temperature and pressure profiles of the chill-down line are measured. The Reynolds numbers vary from 1469 to 5240, which corresponds to the mass flux range of around 19kg/m2s to 49kg/m2s. During the line chill-down process, temperature, pressure, and

mass flow rate are measured. The heat transfer coefficient and the heat flux are then calculated using an inverse problem-solving approach.

Mariano Mercado et al. (2018) presents the results of a deep literature review of 40 studies conducted to gather and consolidate a database of cryogenic flow boiling data in the heating configuration. Design and development of future cryogenic transfer systems depend on accurate correlations for modelling two-phase boiling and heat transfer at low temperatures in both quenching and heating configurations. The goal of this paper is to assess the existing correlations against the gathered experimental data. Twelve sets of data from cryogenic two-phase heated tubes, including 872 nucleate boiling, 2250 film boiling, and 41 data points on critical heat flow, were gathered. A total of 20 heat transfer coefficient and critical heat flow correlations were used to compare the results. The results from cryogenic heated tubes cannot be predicted by the current correlations with any degree of accuracy, although the discrepancy between the data and models is not nearly as great as it is in the quenching arrangement.

Zhang et al. (2019) did "cryogenic quenching enhancement of a nanoporous surface" Surface configuration can improve quenching heat transfer and clear understanding of the effect of different surface characteristics. Investigated is the impact of anodic aluminium oxide (AAO) surface on pool quenching. A theoretical model is used to further explore the impact of surface thermal resistance after quenching the AAO surface and the other four types of surfaces in liquid nitrogen. On the AAO surface, the overall chilldown time is reduced from 63.8 seconds on the electro polishing surface. Due to the phenomena of vapor-filled nanopores, there is less liquid-solid contact surface and a slower rate of local vapour formation, which raises the Leidenfrost point (LFP) temperature and decreases heat flow in the partial nucleate boiling regime. Liquid nitrogen is produced when the surface temperature falls below the crucial pinning state temperature

Gaurav et al. (2019) did "an experimental characterization of the Two Phase (TP) flow characteristics in a horizontal steady state flow of liquid nitrogen" and its subsequent void fraction predictions has been carried out in a novel laboratory set-up. Using a digital imaging equipment, the flow patterns as a function of the relative percentages of liquid and gaseous nitrogen that are externally regulated have been captured, while the temperature and pressure parameters have been captured using the appropriate sensors. According to the starting circumstances, these tests have shown that there are a number

of transitions in the steady state flow of TP nitrogen. Experimental investigation has also been done on the relevant vapour fractions. The Backer's regime map, the regime map provided by Taitel and Dukler, and the Wojtan flow regime map are only a few examples of typical flow regime maps with which the observed flow regimes have been corroborated. The experimentally collected results are shown to be generally converging with the predictions produced from several flow models. These tests should inspire further investigation towards creating a void sensor prototype for cryogenic two-phase flows.

Ran Li et al. (2019) presents "jet impingement boiling heat transfer from rock to liquid nitrogen during cryogenic quenching. The test plate was circular in shape and was 16 cm in diameter and 2 cm in thickness. To emphasise the ways in which the properties of rock material impact the heat transmission from the LN2 jet impingement boiling, a specimen of aluminium alloy with the same configuration as the rock plate was also employed. Rock has a lower heat conductivity than aluminium, and its surface is covered with tiny holes and voids. This surface characteristic allowed the rewetting temperature to increase by 100 °C. The local cold spot idea was used to try to quantify the rewetting temperature improvement. Without film boiling, the stagnation point on the rock surface was directly wetted by an LN2 jet, and it was hypothesised that this was possible due to the high rewetting temperature and quick temperature decrease. For both quenching samples, the maximum heat flux and wetting front velocity were examined, and the findings were compared to relationships in the literature.

Jesna Mohammed et al. (2020) did "an experimental investigations on transient cryogenic chilldown of a short horizontal copper transfer line. The present study investigates chilldown characteristics of a horizontal copper transfer line with 7.94 mm outer diameter, 0.81 mm wall thickness and 500 mm length. The experiments conducted with different mass fluxes (66 kg (m^2.s)$^{-1}$ to 102 kg (m^2.s)$^{-1}$ in a horizontal copper transfer line under terrestrial gravity conditions. A total of six evenly spaced temperature readings were taken, each 330 mm apart from an input. To determine the related heat flux and heat transfer coefficients, inverse problem solving is used. An empirical relation was derived taking into account the quenched wall's thermal characteristics. It is discovered that using copper transfer lines in place of stainless steel transfer lines results in a thermal mass reduction of the section by a factor of 100 and a decrease in the critical heat flux of 50%.

Jesna Mohammed et al. (2020) did “an experimental investigation on heat transfer characteristics in cryogenic chilldown of helically coiled tube. This study focuses on the analysis of heat transmission properties during the cryogenic chilldown of a helical coil. Under conditions of terrestrial gravity, the cryogen was transmitted through copper helical test sections with dimensions of 7.94 mm on the outside, 0.81 mm on the inside, and helix angles of 4, 6, 8, 10, and 16 with horizontal axes, at three different mass fluxes of 66 kg/m2s, 86 kg/m2s, and 102 kg/m2s. Since liquid nitrogen is more readily available and easier to handle than other cryogens, it is used. The findings of obtaining temperature-time connections were compared to those of straight channels. The experiment's findings showed that for a given mass flux, coils with varied helix angles had variable chilldown times. Additionally, chilldown time varied inversely with mass flow for a particular helix angle. Results pointed to the possibility of an ideal helix angle that might help to minimise the chilldown time, hence lowering the use of cryogenic liquid.

2.2 STUDY ON CRYOGENIC CHILLDOWN PROCESS USING THERMAL CONDUCTIVE LAYER

Luca Andena et al. (2004) presented a simulation of PTFE sintering to find the thermal stress and deformational behaviour of both solid (rods) and hollow (billets) blocks. Relevant material parameters were determined experimentally for each stage. Thermo-mechanical analysis was used to comprehensively study the deformation behaviour of PTFE (TMA). Experimental measurements on genuine PTFE-sintered cylinders are compared to the model's predictions. The model's predictions for temperature and deformation distributions are in good agreement with the results of experiments. The impact of cylinder size and applied cooling rate on residual stresses is successfully predicted, and there is good agreement between anticipated and experimentally observed residual stresses.

Daisuke Takeda et al. (2017) presents an experimental method for reducing the time and total mass of cryogenic fluid required for a chilldown process in piping. Polytetrafluoroethylene, which has a low heat conductivity, was applied to the inner wall of a pipe with an outer diameter of 1/4" (=6.35 mm). The pipe was filled with liquid nitrogen (LN2) at a constant tank pressure of 120–170 kPa. The experiment employed a pipe without an insulating layer as well as three additional pipes with insulating layers that were 23 m, 63 m, and 91 m thick, respectively. The two-phase flow's variations,

which were made up of gas phase nitrogen and LN2, were seen. The findings showed that the pipe with the insulating layer had a greater minimum heat flux point (MHF) temperature. The earlier transition began to boil as a result of the higher temperature. Additionally, a maximum of 64% of the total mass of LN2 used in the chilldown procedure might be retrenched. After reaching the MHF point, the heat flux dropped, but it did not significantly affect the total chilldown time. Overall chilldown time is primarily affected by the layer's ability to raise the temperature of the MHF point, which leads to a reduction in both the amount of LN2 used overall and chilldown time.

S. Mohandoss et al. (2017) The present study explain the optimization of applied voltage for deposition of yttria-stabilized zirconia (YSZ) on metal substrate and its electrochemical behavioural studies have become major concern for the preparation of nanostructured zirconia suitable for the realization of dental devices. The electrophoretic deposition (EPD) technique used to apply YSZ coating on 316L SS is described in the current study. The coating range of 60V-70V and coating period of 5 minutes produced the best coatings. The YSZ coated 316L SS samples were sintered at 800°C for 1 hour under vacuum. By using X-ray diffraction, the cubic phase of YSZ coated samples was discovered. The YSZ particles were fairly round and spread evenly over the 316LSS, according to FESEM analysis. Electrochemical methods were used to analyse the anti-corrosion characteristics of the YSZ coated 316L SS samples in artificial saliva solution. The coating of YSZ on the surface of 316L SS is confirmed by the electrochemical results, and it is resistant to a powerful ion assault from fake saliva.

Weitai Xu et al. (2020) did “cryogenic quenching of a stainless steel rodlet with various coating”. It has been known that a thin coating layer with low thermal conductivity on the surface can shorten the quenching time duration. Experiments were carried out by submerging stainless steel rodlets with various coating layers in liquid nitrogen at atmospheric pressure to examine the impact of thin coating layer on cryogenic quenching. In order to assess the impacts of the coating layer's thickness and thermo-physical properties to the quenching performance of the electro-polished surface, two different coating layers of varying thicknesses were created on the surface of the rodlet. It has been demonstrated that a thin coating layer on the rodlet can improve quenching heat transfer efficiency and shorten the overall cooling time. When a theoretical model was used to analyse the mechanism of the improvement of the LFP temperature, it was discovered that even though the average surface temperature is stable and the local surface

temperature is high, the local surface temperature is not high enough to maintain the stability of the local vapour film due to large thermal resistance and small superficial effusivity.

Weitai Xu et al. (2021) did "an experimental investigation of cryogenic flow quenching of horizontal stainless steel tubes. It has been understood in pool quenching experiments that a thin low-thermal-conductive coating layer on the wall can greatly improve the cooling performance, while less is known about the flow quenching. Investigations into the cryogenic flow quenching of horizontal stainless steel tubes with Teflon coating layers on the inner wall are being done in the current study through tests. Three Teflon coating layers of different thicknesses are constructed on the inner wall of stainless steel tubes to study the impact of the coating layer on the quenching performance. The quenching efficiency and quenching heat transfer performance are compared to those of the naked tube. At various input pressures, it is demonstrated that the thin coating layer on the inner tube wall may greatly minimise the quenching time and liquid nitrogen usage. The highest quenching efficiency of the Teflon-coated tube is over 50.0% compared to 8.0% of the bare tube, and the quenching time of the Teflon-coated tube is decreased by up to roughly 78.5%. The sharp temperature drop of the Teflon coating layer surface upon cooling by liquid nitrogen causes the transition boiling with higher heat transfer coefficient to replace film boiling at a higher average wall temperature, resulting in a decrease in quenching time and an increase in quenching efficiency, which is the cause of the improved quenching performance in the current study.

2.3 STUDY ON METHODS USED FOR COATING THE NANO-POWDERS

Sulena Pradhan et al. (2016) in this study, they elucidate the effect of different sonication techniques to efficiently prepare particle dispersions from selected non-functionalized NPs (Cu, Al, Mn, ZnO), and corresponding consequences on the particle dose, surface charge and release of metals. Nanoparticles (NPs) are now used more often in a variety of applications. The recommended technique for distributing the non-inert, non-functionalized metal NPs is probe sonication (Cu, Mn, Al). When sonicating in 1 and 2.56 g/L NP stock solutions, rapid sedimentation during sonication led to discrepancies between the true and given dosages in the range of 30–80%. After sonication, the metal NPs underwent severe agglomeration, which caused all of the particles to silt quickly. These results were corroborated by DLVO simulations, which demonstrated that the strong Vander Waals forces of the metal NPs led to considerable NP agglomeration. Increased sonication resulted in a modest increase in metal release from the metal NPs.

The release of metals in sonicated solutions was accelerated by the addition of a stabilising agent (bovine serum albumin). After 15 minutes of sonication, the degree of particle disintegration for Cu and Mn NPs rose from 1.6 to *5%. The zeta potential of the investigated NPs was little affected by a long sonication time (3–15 min). Overall, it is demonstrated that it is crucial to carefully examine how sonication affects the physicochemical characteristics of disseminated metal NPs. This should be taken into account while studying the nanotoxicology of metal NPs.

Dinesh P.R et al. (2019) studied the fundamentals and application of sonic technology. With the advancement in technology, contaminant removal has become an important factor in many industries. This covers a wide range of industries where defect-free surfaces are regarded vital, such as semiconductor, medical, marine biology, food processing, waste water purification, solar panel cleaning, textile manufacturing, coal washing, optics, and many more. Although there are several wet chemistries for efficient cleaning, companies are always battling to replace the usage of hazardous solvent-based chemistries with eco-friendly cleaning techniques. Researchers have demonstrated that mega Sonics and ultrasonics can successfully replace these wet chemistries, and they are currently widely employed in many different sectors and cutting-edge applications. In order to remove objects, the basic idea behind acoustic cleaning is to employ high-energy sound waves at a frequency higher than human hearing. Surface contamination advancements and removing particle deposits on various structural surfaces The frequency of a sound is commonly used to characterise it and is measured in hertz (Hz), or cycles per second. Humans have a hearing range of 20 Hz to 20 kHz. The "BEL," which bears Alexander Graham Bell's name, is the basic unit of loudness measurement. Decibel (dB), a logarithmic measure of acoustic pressure, is one-tenth of a BEL. The emphasis in sound measurement is on the amplitude of the acoustic pressure, expressed in Pascals (Pa) and/or decibels (dB), and a rise of 10 dB corresponds to a rise in sound pressure of a factor of ten. The movement of particles in a medium, like air or a liquid, allows sound to be transferred.

S Teanmetawong et al. (2019) compared the magnetic stirrer and sonicator technique to disperse 1% span 20 treated Layered Double Hydroxides (LDHs). Layered double hydroxide (LDHs), a 2-dimensional material generated by co-precipitation with an initial particle size of around 100 nm, was studied to determine the effects of particle size reduction and dispersion. To disperse clumped LDHs in a 1 weight percent Span20

solution, which serves as a stabiliser, two basic laboratory dispersing techniques—a magnetic stirrer and sonicator—were used. Agglomerates with single stack LDHs were present in the sonicator product, whereas a cluster of agglomeration particles with better dispersion was visible in the magnetic stirrer.

2.4 RESEARCH GAP

- Many experimental studies are carried out in order to improve the pipe chilldown process.
- Some experimental studies are carried out in order to improve the pipe chill down process using low thermal conducting layer.
- Coating of low conducting material can improve pipe chill down.
- Heat transfer enhancement in cryogenic quenching process with low thermal conducting materials need to be studied.
- Heat transfer study using mixtures of different low thermal conductive powdered materials has not done yet.

2.5 OBJECTIVES

To investigate the effects of the thermo-physical property of the low thermal conductive material coating layer on the stainless steel tube during the quenching process.

- To investigate cryogenic flow quenching of the horizontal stainless steel tube coated with Teflon on the inner walls.
- To investigate cryogenic flow quenching of the horizontal stainless steel tube coated with the YSZ (Yttria-stabilized zirconia) on the inner walls.
- To investigate cryogenic flow quenching of the horizontal stainless steel tube coated with mixture of Teflon and YSZ on the inner walls.
- Comparative and characteristic study of Teflon and YSZ coatings.

2.6 METHODOLOGY

- Literature review
- Analysing the finding of each publications
- Identifying the research gap.

- Problem formulation
- Selection of suitable nano-powders
- Selection of suitable thermocouple
- Experimental setup
- Fabrication of Teflon and YSZ-coated surface
    1. Mechanical Stirring
    2. Sonication
    3. Fill and drain method (paint –epoxy)
- Conduct the experiment to obtain the required parameter.
- Analyse the effect of thermoelectric property of the coating layer on the quenching performance.
- Comparative and characteristic study of Teflon and YSZ coating

CHAPTER 3

CRYOGENIC CHILLDOWN

Boiling curve tests are quite similar to cryogenic chilldown. Precooling or "quenching" cryogenic fluids from room temperature to the fluid saturation temperature is required before introducing them in single phase to the usage point, the transfer line, and related components. Phase shift, two-phase flow boiling, and pressure and velocity changes all occur during the chilldown process. Understanding the boiling phenomena and heat transport regimes can help us learn more in-depth information about this dynamic process. Figure 3.1 provides an example boiling curve illustrating the connection between convective heat flow and wall superheat. For acquiring information on two-phase flow boiling of any fluid, heated tubes or quenching/chilldown experiments are used. Along the previously indicated boiling curve, two alternative routes might happen depending on the approach

Fig 3.1 depicts a typical boiling curve. Almost all chilldown processes begin in the film boiling regime of the boiling curve (Point F) and move towards Point E, then to Points D, C, B, and A, Film boiling occurs when the excess temperature (the difference between the inner wall surface temperature and the fluid saturation temperature) is very large. . During film boiling the surface is not wettable by the liquid, causing a vapor blanket to shroud the surface. During the cooling of the tube wall, heat is transferred from the wall surface to the fluid. A further infusion of cryogen to the wall surface will continue to cool down the surface; eventually allowing the liquid to begin a direct contact with the surface that is called re-wetting. This moment of the first liquid contact is known as the quenching front, and is synonymous with the Leidenfrost point of the boiling curve. The Leidenfrost point is the point of the minimum heat flux in the film boiling regime, marking the onset of the transition boiling regime in a quenching process. During transition boiling, the heat transfer mode is intermittent that results in alternating liquid wetting and vapor drying on the wall surface. Due to the presence of liquid contact, heat transfer is greatly increased. With a decrease in the wall superheat the heat flux increases due to more liquid-to-wall contact. Further cooling of the surface through the transition boiling regime will result in a local peak heat flux termed the critical heat flux (CHF). The CHF point signifies the onset of the nucleate boiling regime and represents the maximum heat flux for the nucleate boiling regime. The chilldown process continues toward point A of Fig 3.1where

boiling (phase change) eventually ceases and single liquid phase convection begins. To chilldown as quickly and efficiently as possible the film boiling regime must be minimized.

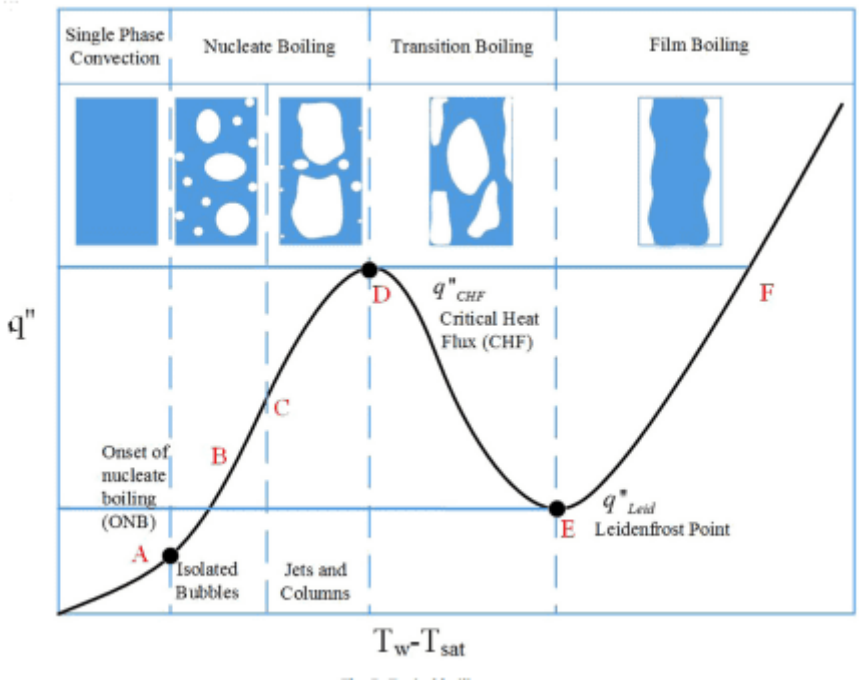

Fig 3.1 Typical boiling curve (Reid Shaeffer et al. 2013)

In tests on steady state boiling, the fluid is heated using a heater. In this case, by altering the heater's external power input, heat flow is kept under control. In contrast, when a fluid is used to quench a wall surface during a test, the process is transitory since the wall superheat and heat flux change with time. The inverse-boiling curve, also known as the chilldown process, starts at the right end of the boiling curve. When liquid is introduced into a test section with a very high wall super heat, the liquid phase instantly evaporates and creates a vapour film, preventing the liquid from coming into touch with the wall. This regime is shown in the movie "Boiling" (F to E). The Leidenfrost point (LFP), or Point E, is the location where there is the least amount of heat transmission from the cold vapour to the tube wall. The liquid phase is able to contact the wall when the LFP is achieved, which is accompanied by intense boiling and a clear drop in wall temperature (rewetting). Transition boiling, which is distinguished from all previous regimes by a high heat flux, is the mechanism of heat transmission at this time. When the liquid makes continuous contact with the wall at the Critical Heat Flux (point D) point, transition

boiling ceases (CHF). Due to the increased volume of liquid coming into touch with the wall surface at this point and the combined sensible and latent heat removal process, heat transfer is at its greatest. As the process moves through points D-C-B, the wall continues to cool, the quality of the vapour declines, the partial nucleate boiling is complete, and the process enters the single phase liquid convection heat transfer regime, signalling the completion of the chilldown process and the beginning of a liquid flow free of vapour. The transition from nucleate two phase cooling to single phase liquid convection occurs at Point B, which is the start of nucleate boiling (ONB).

3.1 CRITICAL HEAT FLUX (CHF)

Critical heat flux (CHF) describes the thermal limit of a phenomenon where a phase change occurs during heating (such as bubbles forming on a metal surface used to heat water), which suddenly decreases the efficiency of heat transfer, thus causing localised overheating of the heating surface.

When liquid coolant undergoes a change in phase due to the absorption of heat from a heated solid surface, a higher transfer rate occurs. The more efficient heat transfer from the heated surface (in the form of heat of vaporization plus sensible heat) and the motions of the bubbles (bubble-driven turbulence and convection) leads to rapid mixing of the fluid. Therefore, boiling heat transfer has played an important role in industrial heat transfer processes such as macroscopic heat transfer exchangers in nuclear and fossil power plants, and in microscopic heat transfer devices such as heat pipes and micro-channels for cooling electronic chips.

The use of boiling is limited by a condition called critical heat flux (CHF), which is also called a boiling crisis or departure from nucleate boiling (DNB). The most serious problem is that the boiling limitation can be directly related to the physical burnout of the materials of a heated surface due to the suddenly inefficient heat transfer through a vapor film formed across the surface resulting from the replacement of liquid by vapor adjacent to the heated surface.

Consequently, the occurrence of CHF is accompanied by an inordinate increase in the surface temperature for a surface-heat-flux-controlled system. Otherwise, an inordinate decrease of the heat transfer rate occurs for a surface-temperature-controlled system. This can be explained with Newton's law of cooling:

$$q = h\,(T_w - T_f)$$

Where q represents the heat flux, h represents the heat transfer coefficient, T_w represents the wall temperature and T_f represents the fluid temperature. If h decreases significantly due to the occurrence of the CHF condition T_w will increase for fixed q and T_f while q will decrease for fixed Δ T.

3.2 LEIDENFROST TEMPERATURE

A certain set of solid-liquid pairs has a feature called the Leidenfrost temperature. The Leidenfrost temperature is the point at which a liquid begins to exhibit the Leidenfrost phenomena on a solid surface. The lowest film boiling temperature of a fluid must be calculated in order to determine the Leidenfrost temperature. Berenson used arguments for the minimal heat flux to derive a relationship for the minimum film boiling temperature. Although the equation for the lowest film boiling temperature, which is contained in the aforementioned reference, is fairly complicated, its characteristics may be comprehended from a physical standpoint. The surface tension is one crucial factor to take into account. Since fluids with higher surface tension require greater amounts of heat flux for the start of nucleate boiling, the proportional connection between the minimum film boiling temperature and surface tension is predicted. The minimum temperature for film boiling should depend proportionally on surface tension since film boiling happens after nucleate boiling.

The Leidenfrost phenomenon is a special case of film boiling, the Leidenfrost temperature is related to the minimum film boiling temperature via a relation which factors in the properties of the solid being used. While the Leidenfrost temperature is not directly related to the surface tension of the fluid, it is indirectly dependent on it through the film boiling temperature. For fluids with similar thermo-physical properties, the one with higher surface tension usually has a higher Leidenfrost temperature.

CHAPTER 4

EXPERIMENTAL INVESTIGATION

4.1 FABRICATION AND CHARACTERIZATION OF THE SURFACE

The stainless steel is widely used in the engineering application and has quite small thermal conductivity, which helps to reduce axial heat conduction. Therefore in the present experiment, the 304L (L – extra low carbon -0.03%) stainless steel tubes are utilized, which are with 8.0 mm diameter, 10 mm outer diameter and 100mm in length.

Fig 4.1 Stainless steel tube (304L)

The inner surface of the steel tubes are coated with low thermal conducting materials like Teflon and YSZ and one other coating is the paint epoxy.

4.1.1 PTFE (Polytetrafluoroethylene) powder

Teflon coatings have a number of properties that make it useful to many industries. PTFE coatings are resistant to corrosive chemicals, provides good insulation from electricity, doesn't absorb water, can withstand extremes of heat and cold, resists UV rays, and creates little friction.

Fig 4.2 Teflon powder (PTFE -Polytetrafluoroethylene)

In addition to its uses in cookware, industrial Teflon coatings are often used in the automotive industry, cabling materials, optical devices, pharmaceutical applications, pipes, valves, and more.

PTFE Micro powder [Polytetrafluoroethylene]	
Product number	NRE-5078
Purity	99.9%
Formula	$(C_2F_4)_n$
Surface area	$17m^2/g$
APS	<40µm
Colour	White
Hardness	50 shore “D”
Melting point	279°C - 326°C
Thermal conductivity	0.25-0.3 W/mK
Density	2200 kg/m^2

Table 4.1 Properties of Teflon powder

4.1.2 YSZ (Yttria-stabilized zirconia) Powder

Yttria-stabilized zirconia (YSZ) is a ceramic in which the cubic crystal structure of zirconium dioxide is made stable at room temperature by an addition of yttrium oxide. These oxides are commonly called "zirconia" (ZrO_2) and "yttria" (Y_2O_3), hence the name.

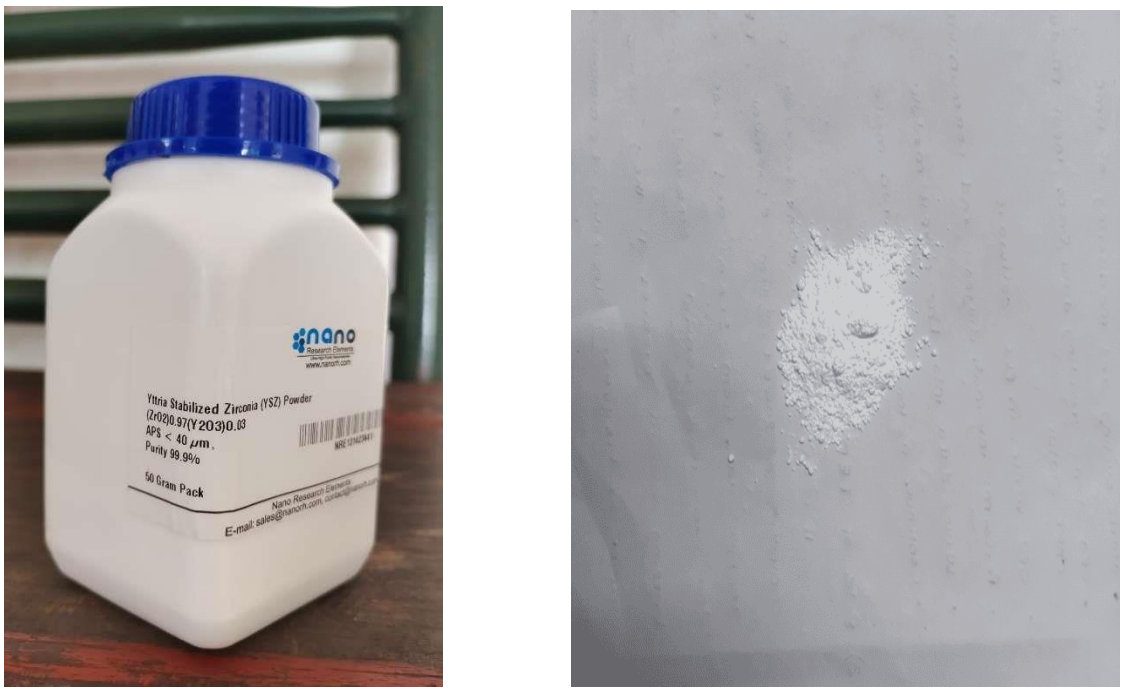

Fig 4.3 YSZ (Yttria-stabilized zirconia)

Thermal barrier coatings (TBCs), which protect metallic components from high-temperature environments, have been widely applied to the fields of high-temperature and corrosion-resistant structural parts such as gas turbine engines, diesel engines, and power generation systems. Yttria-stabilized zirconia (YSZ) is one of the most widely used materials for TBCs owing to its excellent shock resistance, low-thermal conductivity, and relatively high coefficient of thermal expansion.

YSZ has a number of applications:

- For its hardness and chemical inertness (e.g., tooth crowns).
- As a refractory (e.g., in jet engines).
- As a thermal barrier coating in gas turbines.
- As an electro ceramic due to its ion-conducting properties (e.g., to determine oxygen content in exhaust gases, to measure pH in high-temperature water, in fuel cells).

Yttria Stabilized Zirconia (YSZ)	
Product Number	NRE-4026
Formula	ZrO_2 / Y_2O_3
Molecular Weight	349.031g/mol
APS	<40 µm
Purity	99.9%
Colour	White
Melting Point	2600°C
Thermal conductivity	2.2-2.9 W/mK
Density	1.8-2.3 g/cm^3

Table 4.2 Properties of YSZ (Yttria-stabilized zirconia)

4.1.3 Paint epoxy

Epoxy coating is a thick, protective material used to preserve carbon steel tanks from any exterior deterioration. It is well known to be used for industrial concrete floors because of its extreme durability. Epoxy is created by polymerizing a mixture of two compounds, resin and hardener. Once the resin is mixed with a hardening catalyst, the curing process begins. Epoxy coatings provide optimum protection against abrasion, turbulence, corrosive fluids and extreme temperatures. Epoxy coating is not only durable, but also resistant to many corrosive substances. Epoxies are a top choice for many industrial coating applications, including steel, metal, concrete, and more.

Fig 4.4 Paint Epoxy (Grey colour)

Epoxy hardens into a final surface after curing. White enamel paint is typically used by equipment makers since it is less expensive. Tanks painted with enamel paint may require repainting significantly more frequently as a result of corrosion, even indoor tanks. Epoxy coating is not only the most resilient option, but also a green one. Epoxy's strong cohesiveness prevents fumes from eroding or dissolving into the environment, including your air or minute amounts of water. Additionally, using less chemicals overall leads from recoating less frequently.

Because dangerous chemicals are frequently employed for cleaning and machinery operation, chemical corrosion is a problem in industrial operations. Because it will shield your tank from these harmful substances, an epoxy coating is appropriate

4.2 CALCULATION

Equation

1. Volume of tube (inner surface)

Volume = $\frac{\pi}{4} D_i^2$ L

$=\frac{\pi}{4}$ $(8)^2 100$

$= 5.026\times10^{-6}$ m^3

2. Mass = volume × Density

- Teflon

Density of Teflon = 2200 kg/m3

Mass of Teflon = 5.026×"10−6"× 2200

= 0.0110kg

= 11.05 g

50% of Teflon powder is 5.5 g

60% of powder is 6.6 g

- YSZ

  Density of YSZ = 1800 kg/m3

  Mass of YSZ = 5.026×"10−6"×1800

  = 9.046 ×10-3 kg

  = 9.04 g

  50% of YSZ powder is 4.5 g

  60% of YSZ powder is 5.4 g

- Teflon-YSZ mixture

  50% of mixture is 10 g

  60% of mixture is 12 g

4.3 METHODS OF COATING

To understand the mechanism of the quenching enhancement incurred by thermo-physical property and thickness of the coating layers are fabricated on the stainless steel rodlet. Specifically two Teflon coated, two YSZ-coated and two Teflon-YSZ coated inner surface with different thickness. Here the nano powders are mixed with paint epoxy. Therefore the preparation of coating layer consists of the following steps:

4.3.1 Mechanical stirring

Stirring is a method to obtain homogeneous mixtures and (or) intensify heat and mass exchange in the mixers. In accordance with the state of aggregation of matter there is a mixing of liquids and bulk solids. Stirring is carried out mainly in the vessels with mixing devices. The nature and intensity of mixing depends on the design of devices and mixers. Magnetic stirring can be used over a broad temperature range and with any chemical agent, as well as in open and closed systems, under pressure or vacuum.

Magnetic stirrers are used to do the most typical mixing. Two primary components make up the apparatus: a motor with a stirring mechanism and control electronics. Stir bars rotate as a result of a motor's top-mounted magnet, mixing the liquids. Control electronics monitor keyboard and motor RPM.

Magnetic stirrers are designed for mixing fluids of different viscosity with the help of a stir bar that spins very quickly. They are commonly used for sample preparation and analysis, in chemistry, biology and in such laboratory works as organic synthesis, extraction, oil analysis, pH measurement, dialysis, soil suspending, preparing buffer

solutions where it is often needed to mix several types of liquids to get homogeneous mixtures. Magnetic stirrers have different service performance and technical parameters. The main difference is in the design which means that mixing occurs by rotating or oscillating processes. When you choose a magnetic stirrer you should take into consideration the volume of the liquid container, the speed of rotation, the oscillation intensity and heating if you need to raise the temperature of the mixture.

Fig 4.5 Magnetic Stirrer

A magnetic stirrer is an electro mechanical device that mixes with the help of an external magnetic field that rotates a stir bar placed in the mixture. Stir bar rotates at different speeds and can mix volumes up to one litre. Since only a small magnet bar which can easily be cleaned and sterilized has to be put inside the sample, the risk of contamination is minimized. Magnetic stir bars work well in glass vessels. Glass is the material that doesn’t affect a magnetic field.

Here the paint epoxy and nano-powders are mixed in a glass beaker with the help of magnetic stirrer. The coating of the pipes are as follows:

Mixing of paint epoxy with Teflon

Teflon and epoxy are mixed in a glass beaker with the help of a magnetic stirrer for 400 rotations. It rotates for 15 minutes.

- First mixing with 5.5 g of Teflon powder and 15 ml of Epoxy.
- Second mixing with 6.6 g of Teflon powder and 20 ml of Epoxy.

Mixing of paint epoxy with YSZ

YSZ and epoxy are mixed in a glass beaker with the help of a magnetic stirrer for 400 rotations. It rotates for 15 minutes.

- First mixing is with 4.5 g of Teflon powder and 15 ml of Epoxy.
- Second mixing is coated with 5.4 g Teflon powder and 20 ml of Epoxy.

Mixing of paint epoxy with the mixture of Teflon and YSZ

Teflon –YSZ mixture and epoxy are mixed in a glass beaker with the help of a magnetic stirrer for 900 rotations. Because the mix is very thick and it rotates for 15 minutes.

- Firs mixing with 10 g of mixture and 30 ml of epoxy.
- Second mixing with 12 g of mixture and 35 ml of epoxy.

4.3.2 Sonication

The sonication process uses ultrasonic sound waves. During the process, there is a production of thousands of microscopic vacuum bubbles in the solution due to applied pressure. The formed bubbles collapse into the solution during the process of cavitation.

In the cavitation field, bubbles collapse, creating waves in the process that releases a tremendous amount of energy. The molecular connections between the water molecules are broken down as a result. The molecular connections decrease, which causes the particles to start separating and allowing the mixing process to happen. The sound waves release energy, causing friction in the solution as a result. To keep the sample from heating up during and after the sonication procedure, ice cubes are utilised.

Fig 4.6 Sonicator

Sonication is widely used in the laboratory to disperse nanopowders into the polymer matrix.In this procedure, the nanoparticles in the polymer matrix are stirred up using ultrasonic radiation. Typically, an ultrasonic bath or horn/probe, sometimes referred to as a sonicator, is used to perform it. The typical duration of sonication or shaking is 15 to 1 minutes. A strong piece of laboratory equipment called a sonicator generates an ultrasonic electric signal that powers a transducer. Using piezoelectric crystals, or crystals that immediately respond to electricity by producing a mechanical vibration, this transducer translates the electric signal.

Fig 4.7 Sonication of the mixtures

Here for the complete mixing of nanopowders and paint epoxy we are using sonicator. The sonication process helps to complete and thorough mixing of the mixtures. During sonication the temperature of water increases. We set the temperature at 30°C and it increases to 40° C. The sonication time for this mixing is 5 minutes.

4.3.3 Fill and Drain method

Fill and drain method of coating is conceptually accepted method by ISRO. Close the one end of the sample tube and hold the tube perpendicularly. Then fill the solution of nanopowder and epoxy inside the sample tube as shown in the fig 4.8 (a) and (b). Hold the sample tube for 2-3 min and then gently drain the extra solution from the tube completely and remove the covering and let it dry. It will take 2-4 hours for complete settle of the solution.

(a)

(b)

Fig 4.8 (a) and (b) Fill and Drain method

Filling and draining of each solution:

Uncoated pipe

One pipe is kept uncoated. In order to compare the quenching performance of the coated rodlets with that of the bare rodlets was also fabricated.

Epoxy coated pipe

10 ml of paint epoxy is filled inside the pipe by using fill and drain method and kept it for 3-4 hours and let it dry without any disturbance

Two pipe coated with Teflon

After sonication process the completely mixed solution is filled inside the pipe. First pipe coated with 5.5 g of Teflon powder and 15 ml of Epoxy and the second pipe coated with 6.6 g of Teflon powder and 20 ml of Epoxy by filling and drain method.

Two pipe coated with YSZ

By using fill and drain method the solution of YSZ and paint epoxy after sonication is filled inside the pipe. First pipe coated with 4.5 g of Teflon powder and 15 ml of Epoxy and the second pipe is coated with 5.4 g Teflon powder and 20 ml of Epoxy and let it dry for 3-4 hours.

Two pipe coated with mixture of Teflon and YSZ

The thermal conductivity of Teflon very low and YSZ is used for thermal barrier.so we mix the Teflon and YSZ powder, together they form a strong barrier. First pipe is coated with 10 g of mixture and 30 ml of epoxy and second pipe is coated with 12 g of mixture and 35 ml of epoxy by fill and drain method after completely mixing of the powders and epoxy by sonication.

4.4 EXPERIMENTAL PROCUREMENTS

The instruments and devices used for the experiment are discussed below

4.4.1 Thermocouples

T-type thermocouples were used to measure the outer wall temperature of the pipe. Twelve, T-type thermocouples were used. They have high stability at sub- zero temperatures. In T- type thermocouple positive leg is composed of copper and negative leg consist of mixture of 55% copper and 45% nickel which is known as constantan. Temperature range: -270 to 370°C.

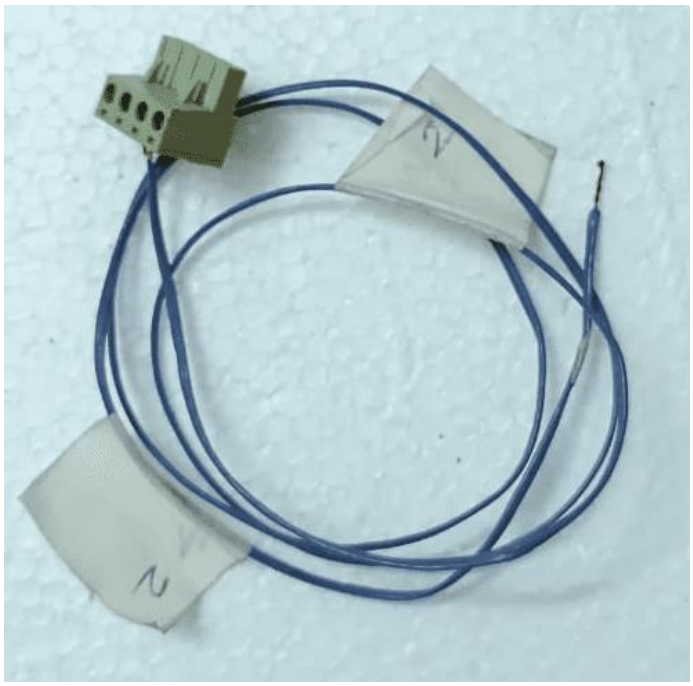

Fig 4.9 T-type thermocouple

4.4.2 Liquid nitrogen (LN_2)

Liquid nitrogen (LN2) is nitrogen in a liquid state at low temperature. Liquid nitrogen has a boiling point of about −195.8 °C (−320 °F; 77 K). It is produced industrially by fractional distillation of liquid air. It is a colourless, low viscosity liquid that is widely used as a coolant**.**

Liquid nitrogen is a compact and readily transported source of dry nitrogen gas, as it does not require pressurization. Liquid nitrogen possesses many desirable characteristics like non-corrosiveness, chemical inertness, ease of availability, non-flammability and cheaper cost and hence a mong the research community in chilldown studies. favourite Further,

its ability to maintain temperatures far below the freezing point of water makes it extremely useful in a wide range of applications, primarily as an open-cycle refrigerant, including:

- In cryo-therapy for removing unsightly or potentially malignant skin lesions such as warts and actinic keratosis
- To store cells at low temperature for laboratory work
- in cryogenics
- In a cryo-phorus to demonstrate rapid freezing by evaporation
- As a backup nitrogen source in hypoxic air fire prevention systems
- As a source of very dry nitrogen gas
- For the immersion, freezing, and transportation of food products
- For the cryopreservation of blood, reproductive cells (sperm and egg), and other biological samples and materials
- To preserve tissue samples from surgical excisions for future studies
- To facilitate cryo-conservation of animal genetic resources

4.4.3 Polyurethane foam

Insulation made of polyurethane foam is offered in both closed-cell and open-cell varieties. In addition to being used to insulate hollow walls, polyurethane foam may also be utilised to insulate floors, pipes, and industrial systems. Using PUR-made insulating panels, the whole building envelope may be covered. Another noteworthy aspect is that PUR may be injected into existing hollow walls utilising the existing apertures and a little extra hole. In general, the basis for thermal insulation is the very low heat conductivity of gases. Gases are good insulating materials if they can be confined since they have low thermal conductivity compared to liquids and solids (e.g., in a foam-like structure). Other gases, including air, also perform well as insulators. However, the main benefit is the absence of convection. In order to prevent large-scale convection, many insulating materials, such polyurethane foam, simply include a number of gas-filled pockets. Due to the interchange of gas pockets and solid materials, heat must be transferred over several surfaces, which causes a rapid decline in the heat transfer coefficient.

4.4.4 Data Acquisition System

The keysight-34992A Data Acquisition Unit collects and stores data from sensors that are attached to it. The data logger's software converts mill volt signals from thermocouples to temperature data directly .Data can be transferred from the software's native file format to the Microsoft Excel platform.

Fig 4.10 Data acquisition system

4.5 EXPERIMENTAL SET-UP

The schematic diagram of the experimental apparatus is illustrated in fig 5.1. It mainly composed of a LN_2 supply tank (Dewar vessel), a sub-cooler, a bypass line and a test section. Liquid nitrogen is supplied by a self-pressurized supply tank and pass through a sub-cooler. The sub-cooler is installed in front of the test line in order to cool down the partially vaporized liquid nitrogen in the transport line from LN_2 supply tank .The sub-cooler is fabricated by a copper tube. A bypass valve is set upstream the entrance of the tube to ensure that only liquid nitrogen enters the tube. To reduce the heat leak, the tube is wrapped with poly-urethane thermal insulation material.

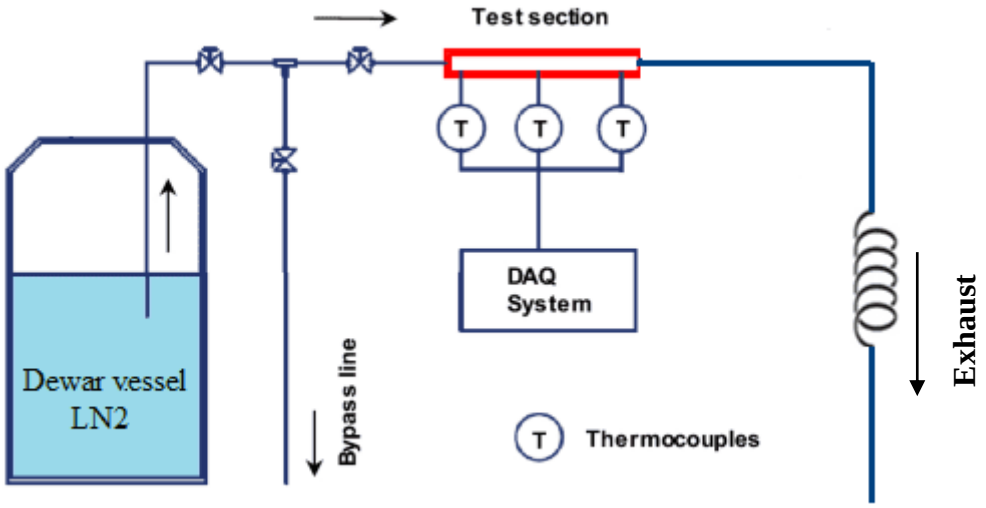

Fig 4.11 Schematic diagram of experimental apparatus for cryogenic line chill-down (Jesna Mohammed et al.2020)

The detailed information of the test section and the installing location of the sensors are depicted in fig 5.4 and fig 5.5. The specifications of the test section are listed in table 5.1. The test line is 10 cm long stainless steel. The outer diameter of the pipe 10 mm and inner diameter of the pipe is 8 mm. The heat in-leak to the test section was minimised using polyurethane foam insulation. Pre calibrated T-type thermocouples tied onto the tube surface using a thin copper wire. The output of all sensors was read by Keysight 34972A data acquisition system.

Specification	**Pipe**
Material	Stainless steel 304L
Outer diameter	10mm
Inner diameter	8mm
Length	100mm
Thermal insulation	polyurethane foam
Thermocouple	T-type (12 nos)

Table 5.1 specification of test section

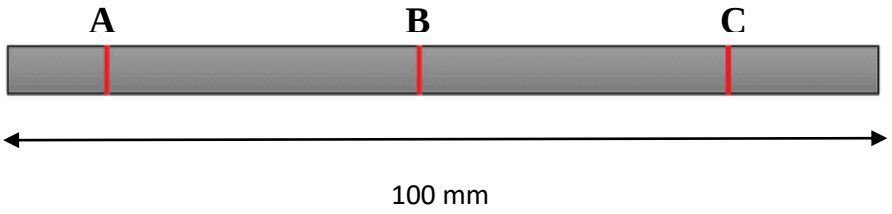

Fig 4.12 schematic illustration of test sample

On each cross-section at three location A, B and C of the pipe along the flow direction, temperature measurement points were set at the top, bottom and each sides as shown in fig 5.5.

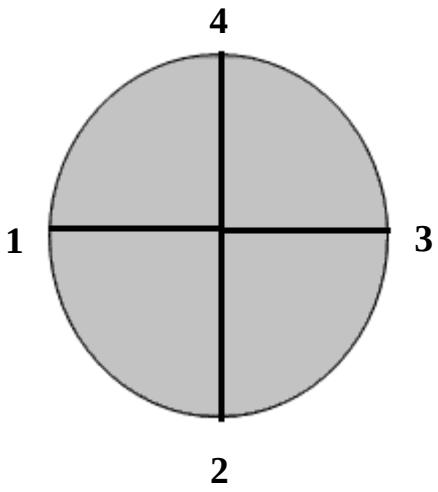

Fig 4.13 Cross sectional (enlarged).

4.6 EXPERIMENTAL PROCEDURE

Fig 5.6 shows the experimental system. The chill-down experiment consists of two parts:

1) Precooling process of the LN_2 -transport line from LN_2 supply tank to the inlet of the test line and sub-cooling of LN_2 at the inlet position of test line.

The initial temperature of the whole system is at room temperature and the initial pressure is at atmospheric pressure. Valve 1 is maintained open during the whole process. Firstly, the bypass valve, valve 3 is opened and the test section valve, valve 2 is closed. LN_2 from the supply tank passes and cools down the transport line. The vaporized LN_2 passes

through the bypass line until the inlet fluid temperature of the test line, $T_{f\,in}$, reaches the sub-cooled temperature under the inlet pressure of the test section, P_{in}.

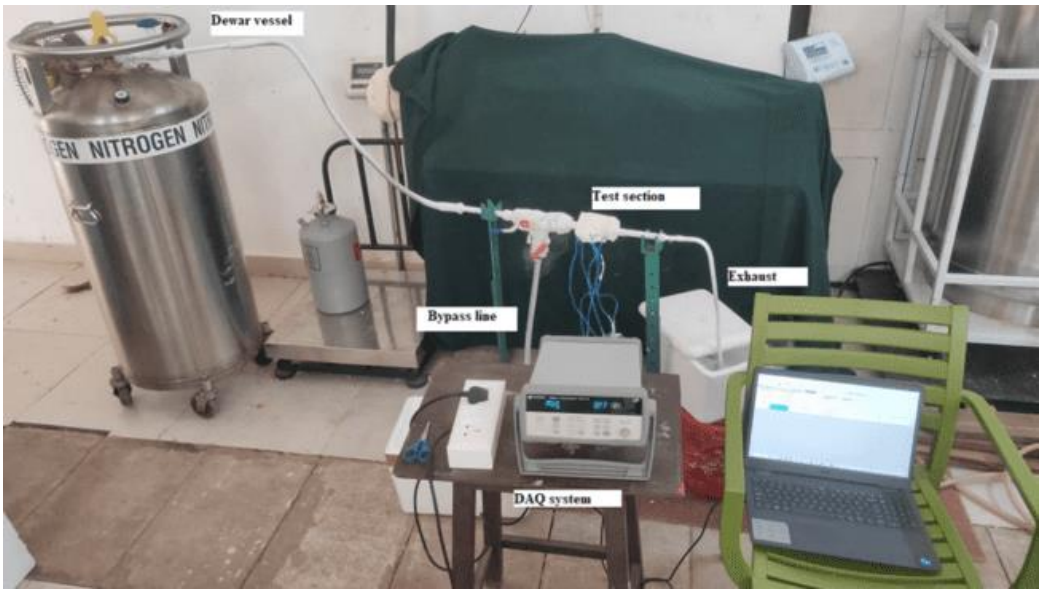

Fig 4.14 Experimental setup for chilldown study

2) Chill-down process of the test line.

The test line chill-down process is started by closing valve 3 and simultaneously opening the valve 2. This was used to ensure the entry of single phase liquid nitrogen into the test section. The wall temperature measurements were recorded at three equidistant points.

The major source of uncertainty in measurements was from the temperature measurement from thermocouples, DAQ. An uncertainty of ±1 K is to be expected from temperature measurements. The experiments in each input condition were conducted thrice for ensuring repeatability.

4.7 MEASUREMENT AND DATA REDUCTION

4.7.1 Inner wall temperature, heat flux and heat transfer coefficient evaluations

To understand the heat transfer characteristics of the flow quenching, the establishment of the quenching curve is necessary. However the direct measurement of inner wall temperature is impractical. Here the outer wall temperature is measured and both the inner wall temperature and heat flux were estimated based on the measured temperatures on the outer surface of the tube. Burgraff ‘s correlations for the determination of inner wall

temperature, Ti and heat flux, qi". The method is based on lumped capacitance analysis and can produce accurate results using fewer terms. The model neglects axial heat transfer along the test section.

Inside wall temperature can be given by the correlation:

$$T_i = T_o + \left\{\frac{r_o^2}{4\alpha}\left[\left(\frac{r_i}{r_o}\right)^2 - 1 - 2ln\left(\frac{r_i}{r_o}\right)\right]\right\}\frac{dT_o}{dt} + \left[\frac{1}{64\alpha^2}(r_i^4 - 5r_o^4) - \frac{r_o^2 r_i^2}{8\alpha^2}ln\left(\frac{r_i}{r_o}\right) - \frac{r_o^4}{16\alpha^2}ln\left(\frac{r_i}{r_o}\right) + \frac{r_o^2 r_i^2}{16\alpha^2}\right]\frac{d^2T_o}{dt^2}$$

And inner wall surface heat flux can be calculated with the equation

$$q_w'' = \rho c_p\left(\frac{r_i^2 - r_o^2}{r_i}\right)\frac{dT_o}{dt} + \frac{(\rho c_p)^2}{k}\left[\frac{r_i^3}{16} - \frac{r_o^4}{16r_i} - \frac{r_o^2 r_i}{16}ln\left(\frac{r_i}{r_o}\right)\right]\frac{d^2T_o}{dt^2} + \frac{(\rho c_p)^3}{k^3}\left[\frac{r_i^5}{384} - \frac{3r_o^4 r_i}{128} + \frac{3r_o^2 r_i^3}{128} - \frac{r_o^6}{384r_i} - \frac{r_o^2 r_i^3}{128}ln\left(\frac{r_i}{r_o}\right) - \frac{r_o^4 r_i}{32}ln\left(\frac{r_i}{r_o}\right)\right]\frac{d^3T_o}{dt^3}$$

The parasitic heat load present through the insulation provided can be calculated as:

$$q''_{parasitic,o} = q''_{cond,o} + q''_{conv,o} + q''_{rad}$$

As the temperature difference between the surface of the insulation and surrounding was negligible, the convective and radiative heat transfer at the surface of the insulation can be neglected.

$$q''_{cond,o} = -\left(kA\frac{\partial T}{\partial x}\right)$$

Thus,

Net heat transfer at inner wall can be calculated as:

$$q'' = \frac{r_o}{r_i}\left(q''_{parasitic,o}\right) - q''_i - q'_a$$

In chilldown processes the axial conduction heat transfer, q_a" is normally considered as negligible.

Heat transfer coefficient can be found using the equation

$$h_i = \frac{q''}{(T_i - T_{sat})}$$

Inner wall temperature profile was found to have small or negligible variation from the outer wall profiles. This may be due to the small thickness and high thermal conductivity of the test section.

The physical properties of stainless steel pipe significantly vary from the room temperature to the cryogenic temperature, and the saturation temperature of nitrogen also depends on the pressure which are not negligible in calculation. Nitrogen and stainless steel pipe properties used for calculation as follows:

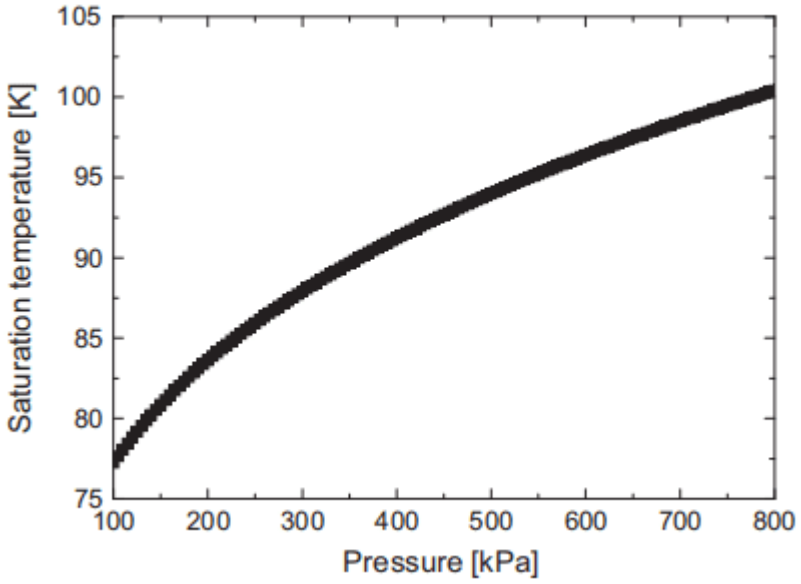

Fig.4.15 Saturation temperature curve of nitrogen gas (Jin et al. 2016)

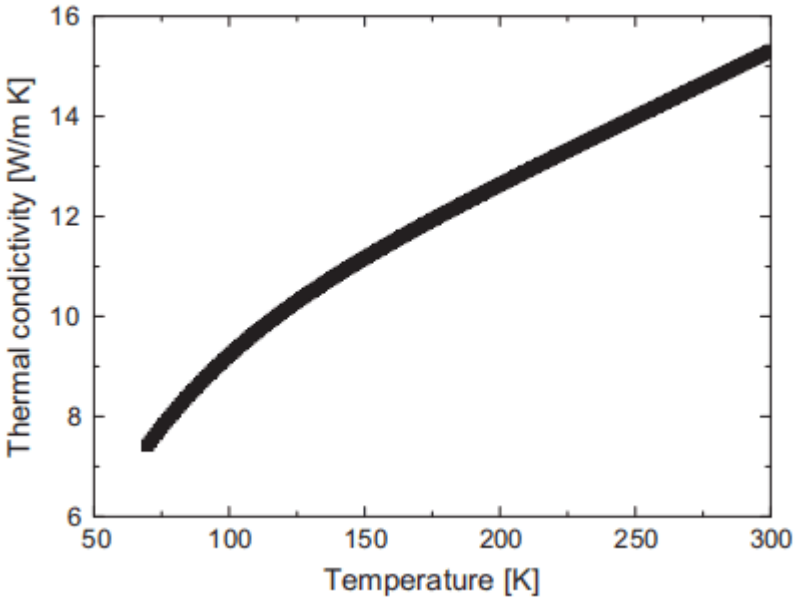

Fig.4.16 Thermal conductivity of stainless steel 304 versus temperature. (Jin et al. 2016)

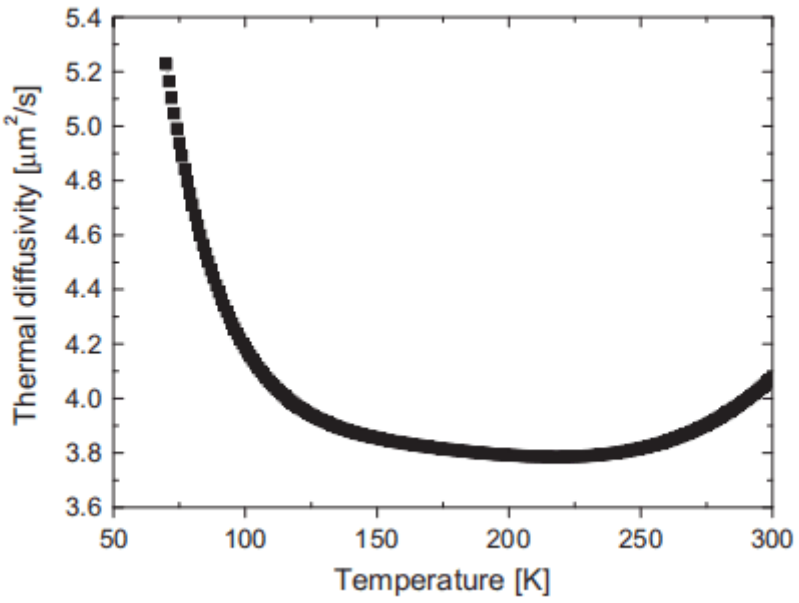

Fig.4.17 Thermal diffusivity of stainless steel 304 versus temperature. (Jin et al. 2016)

CHAPTER 5

RESULT AND DISCUSSION

5.1 IMPROVEMENT OF FLOW QUENCHING PERFORMANCE BY THE COATING LAYERS

The cooling curve of the outer wall shows the variation of temperature with time during quenching process, as shown in below Figures. It should be noted that the top wall temperature of the tube is generally the highest, followed by the side and bottom temperatures due to the effect of gravity on the flow patterns in horizontal tube. The temperature of the outer wall is always higher than that of the inner wall during quenching process. Therefore, the time required for the outer bottom wall temperature near the outlet of the tube to decrease to the steady temperature can be regarded as the entire quenching time of the tube. Thus, the outer top wall temperature at location A (bottom) is used as the reference to characterize quenching process**.**

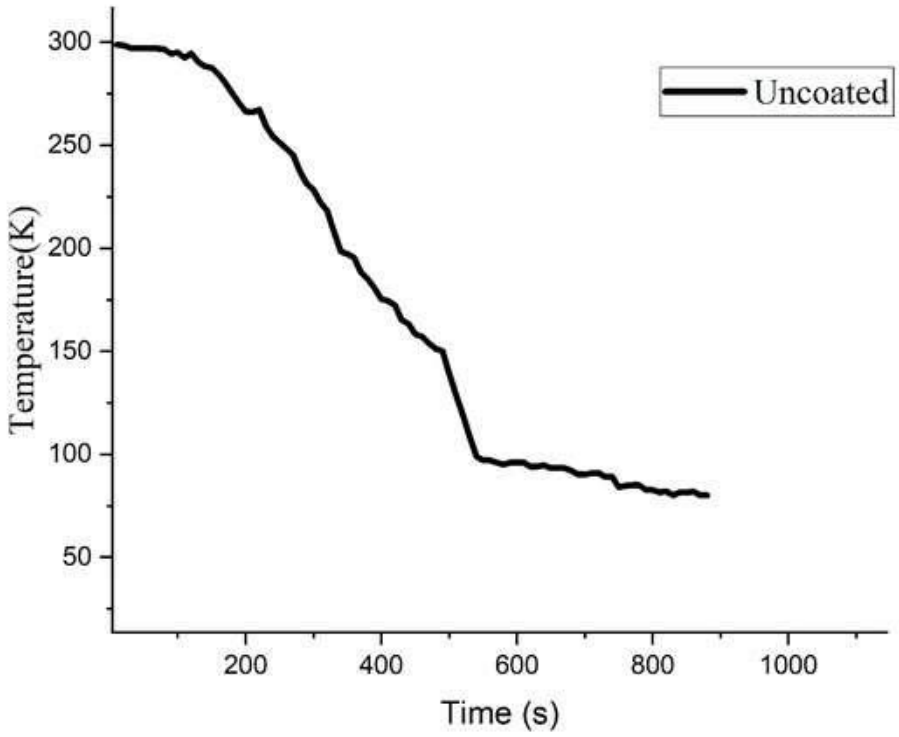

Fig 5.1 Variation of temperature with time (uncoated)

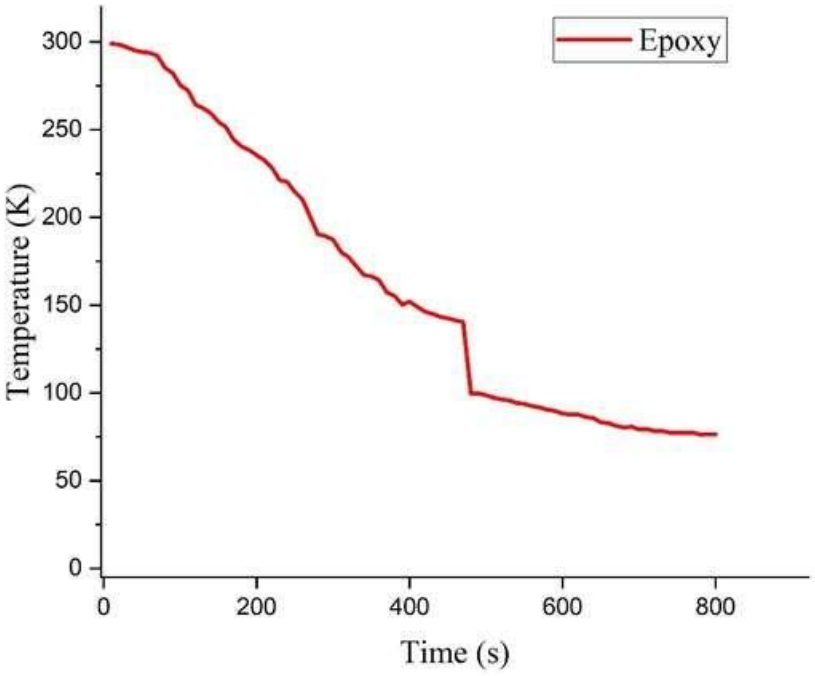

Fig 5.2 Variation of temperature with time (epoxy coated)

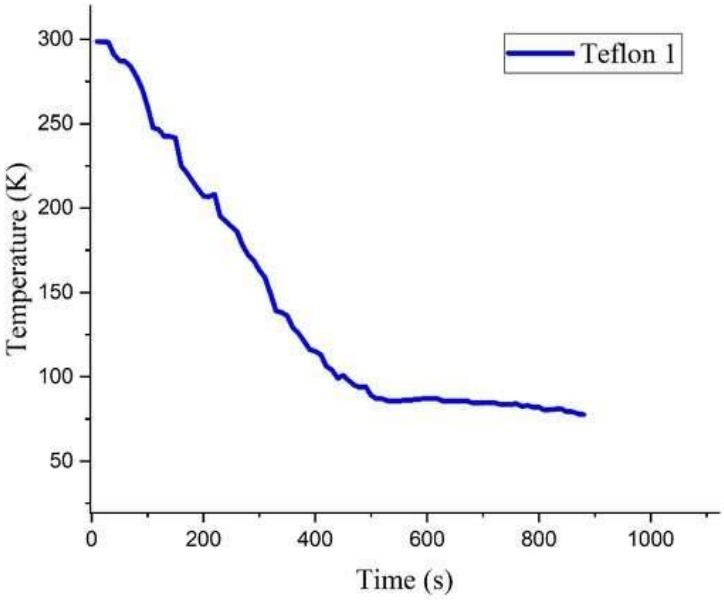

Fig 5.3 Variation of temperature with time (Teflon 1- 50%)

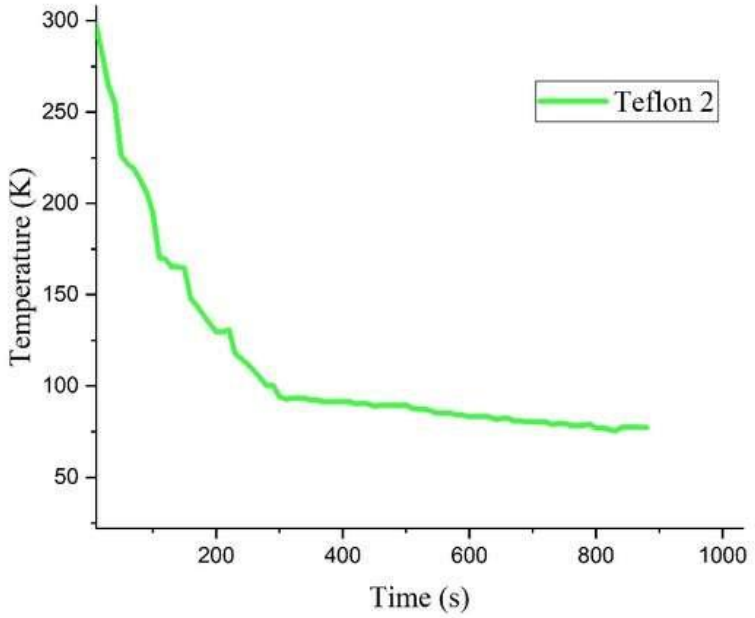

Fig 5.4 Variation of temperature with time (Teflon 2-60%)

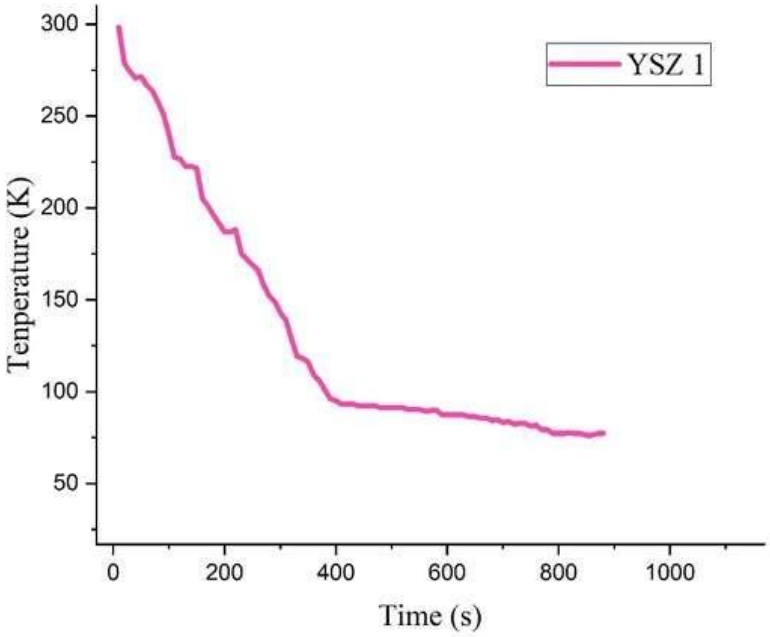

Fig 5.5 Variation of temperature and time (YSZ 1-50%)

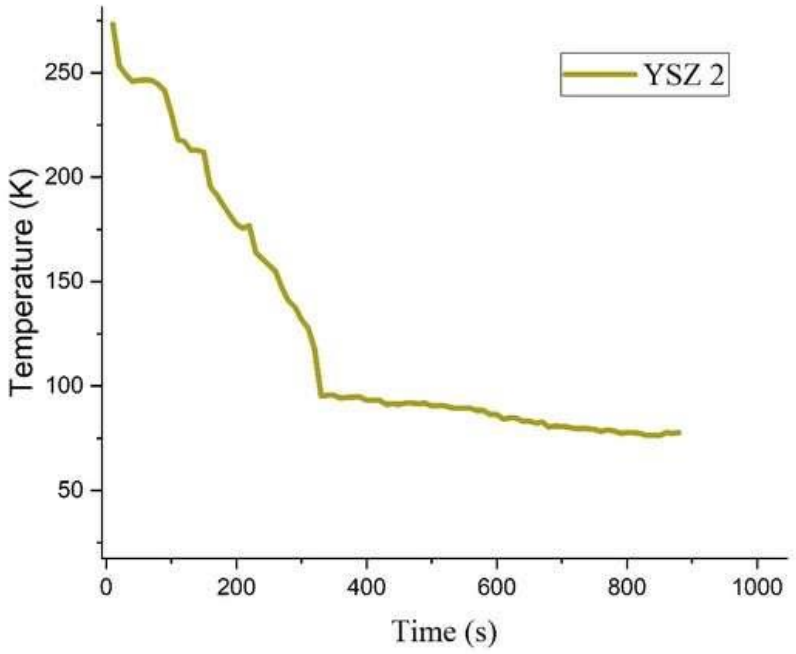

Fig 5.6 variation of temperature with time (YSZ 2-60%)

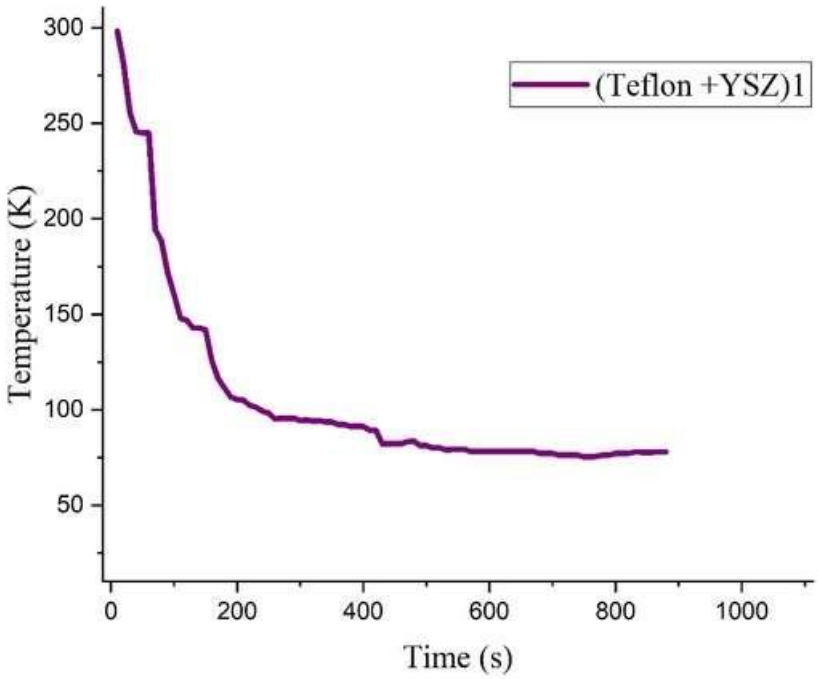

Fig 5.7 variation of temperature with time (Teflon and YSZ) 1

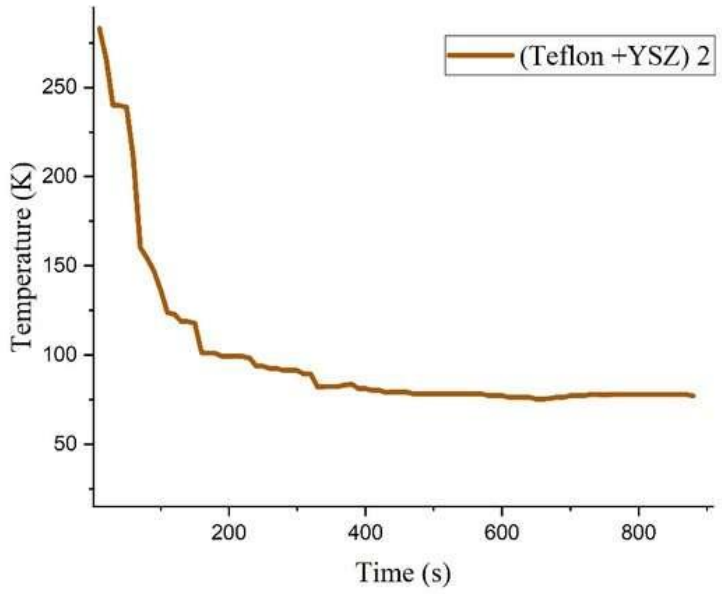

Fig 5.8 variation of temperature with time (Teflon and YSZ (2))

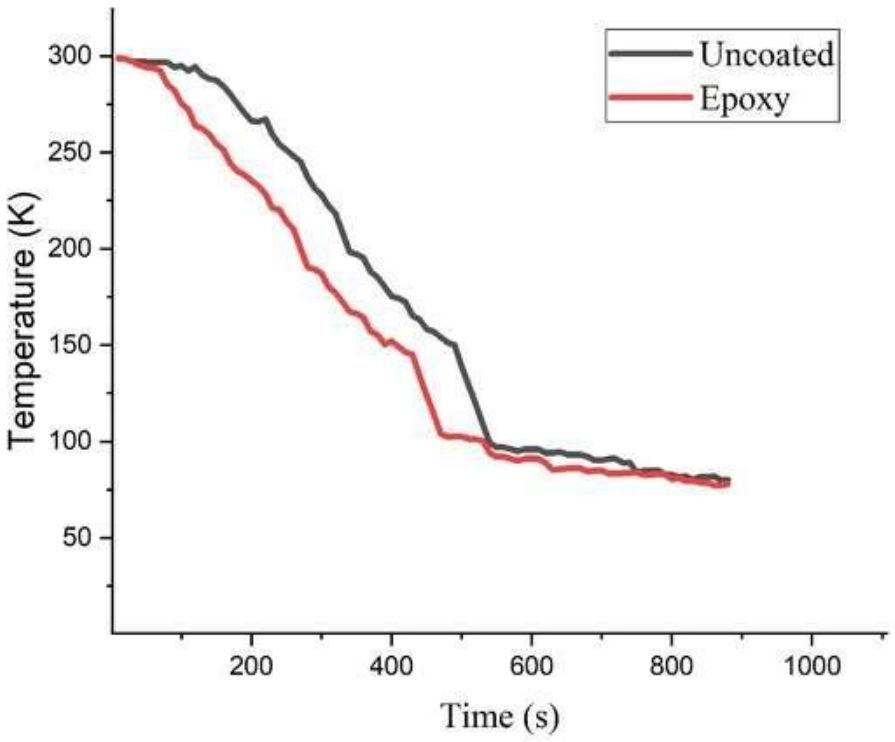

Fig 5.9 comparison of uncoated and epoxy surfaces

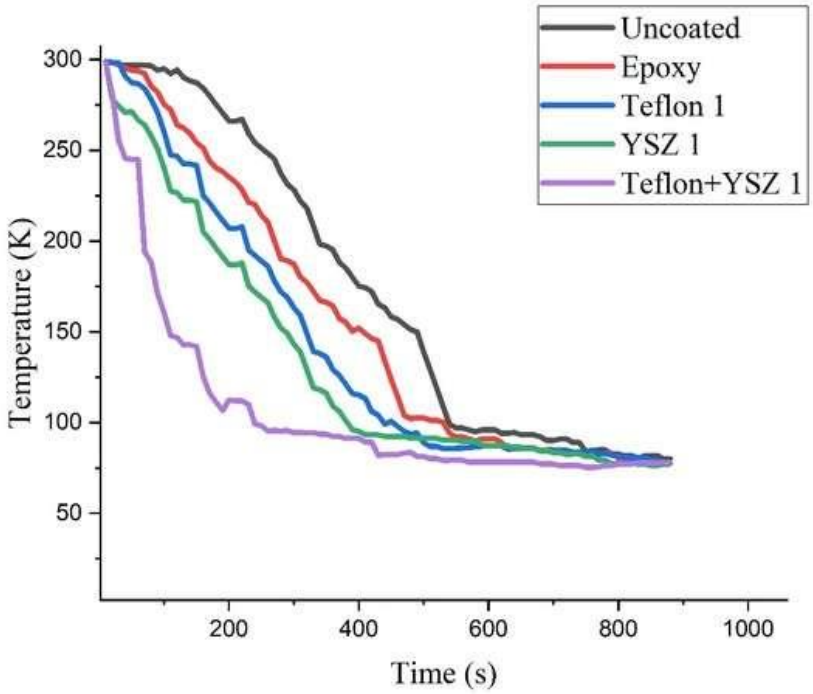

Fig 5.10 Comparison of uncoated and coated surface (50% powder coated surfaces)

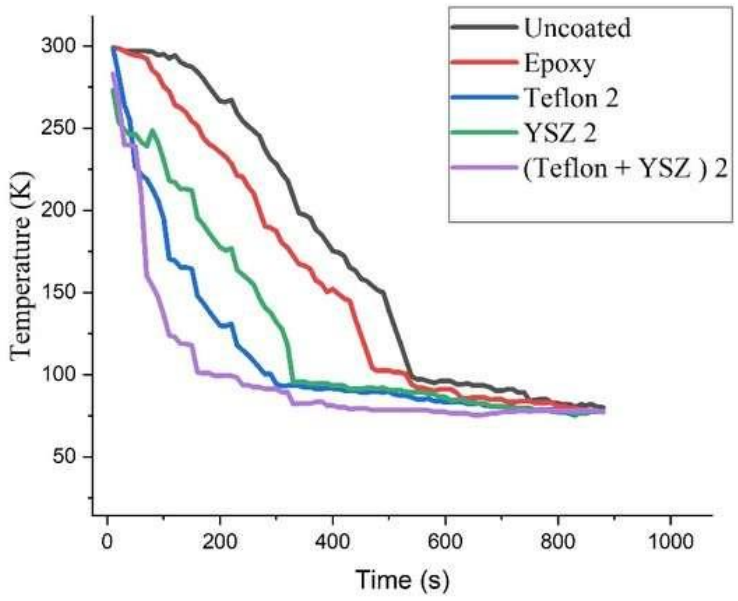

Fig 5.11 Comparison of uncoated and coated surfaces (60% powder coated surfaces)

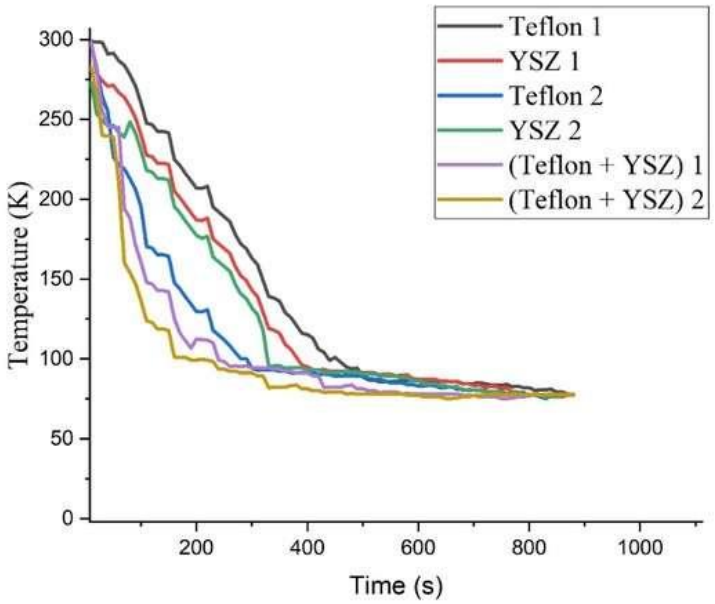

Fig 5.12 Comparison of coated surfaces

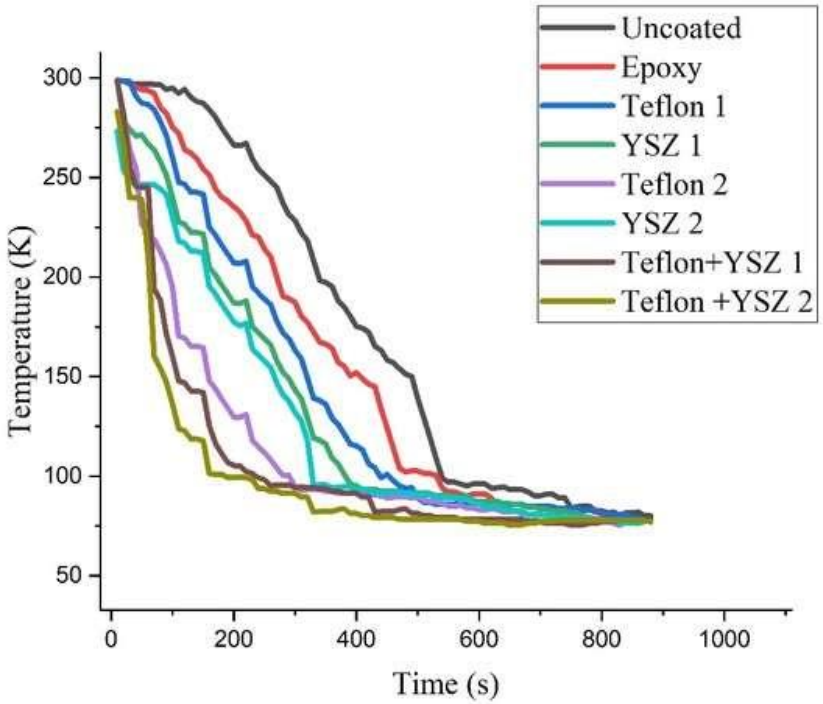

Fig 5.13 Comparison of uncoated with coated surfaces

The measured temperatures of eight samples at the inlet pressure of 20 Psi are selected as examples to display the quenching characteristics, as shown in Fig. 5.11. It is seen that the distinct differences among the curves can be identified and there is an apparent slope change from about 130 K at nearly 500 s in the temperature curve of the bare tube, where the inflection point is the LFP, indicating the conversion of film boiling to transition boiling on the inner wall. While in the curves for the Teflon-coated tubes, the film boiling vanishes due to the presence of the Teflon coating layer and the temperatures of the tubes drop very fast. Compared with the quenching time of about 500s for the bare tube, the quenching times for the epoxy, Teflon-coated, YSZ-coated, and companied coated are about 415s, 375s, 125s, 315s,225s, 115s s and 105 s, respectively, as the thickness of the coating layer increases. The bare tube experiences the longest quenching time due to the longest film boiling stage, as shown in Fig. 6.11. The low-thermal-conductive coating layer on the inner tube wall shortens the quenching time significantly and the larger the thickness, the shorter the quenching time.

5.2 INNER WALL TEMPERATURE, HEAT FLUX AND HEAT TRANSFER COEFFICIENT EVALUATIONS

To explain the mechanism behind the phenomenon, we analyze the surface heat transfer characteristics according to results obtained by the inverse heat transfer analysis discussed above in this section. From the surface temperature curves of the YSZ coated, there are apparent slope changes of all the curves. At the beginning, the temperatures of the surface decrease slowly with slight differences among all the curves due to the stable film boiling, where the surface is covered by a stable vapor film. When the heat transfer mode changes from film boiling to transition boiling, the surface temperature decreases sharply at the LFP, at which the slope of the quenching curve changes. Ahead of the LFP, boiling mode is film boiling with poor heat transfer performance. Afterwards, the boiling mode enters transition boiling and nucleate boiling with a greater cooling rate (slope of the quenching curve) as the surface temperature decreases. As shown in Fig. 6.11 the LFP temperature is improved with the increase of the thickness of coating layer, which allows the boiling mode to enter the transition boiling and nucleate boiling earlier at higher temperature. The shortening of the film boiling regime and the extension of the transition boiling regime and nucleate boiling regime improves the total heat transfer, thus shortening the quenching time duration.

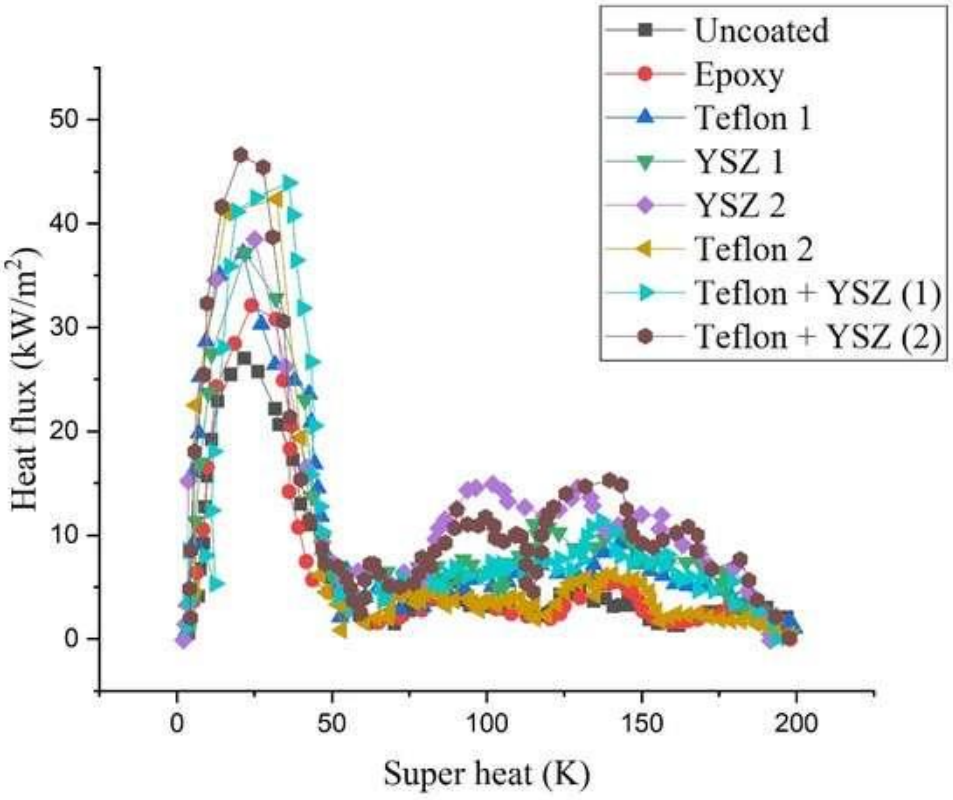

Fig 5.14 Variation of heat flux with wall superheat.

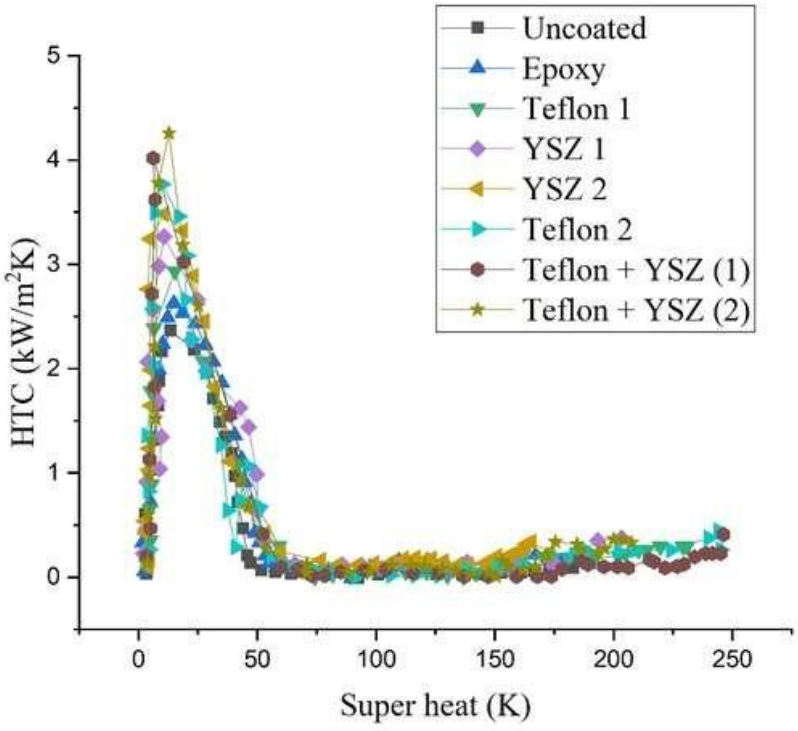

Fig 5.15 variation of heat transfer coefficient with superheat

Surface	**Cooling Time Duration (s)**	**Heat Flux (kW/m^2)**	**Heat Transfer Coefficient (kW/m^2K)**
Uncoated	500	28	2.42
Epoxy	415	32	2.64
Teflon 1	325	34	2.88
YSZ 1	315	36	3.22
Teflon 2	125	43	3.68
YSZ 2	225	38	3.39
(Teflon +YSZ) 1	115	45	4.11
(Teflon + YSZ) 2	105	48	4.48

Table 5.1 The cooling Time Duration, Heat flux, Heat Transfer Coefficient

Fig.5.10 shows the variation of 50% powder coated surface and uncoated surface, where the quenching time of YSZ is less compared to Teflon. Fig 5.11 shows the variation of 60% powder coated surface and uncoated surface, where the quenching time of Teflon is less compared to YSZ. In both cases of mixture of Teflon and YSZ coated surface, shows less quenching time. As the thickness of Teflon increases quenching is reduced.

Fig. 5.14 shows the heat flux versus surface superheat of the coated surfaces, where surface superheat is defined as the difference between the surface temperature and saturated temperature of liquid nitrogen. Fig. 5.14 shows the computed results of the total inner wall heat flux, q_i'', and the flow boiling HTC in location A as a function of the temperature differences between pipe inner wall and fluid. Both heat flux and the heat transfer coefficient curves are almost overlapped. As shown in Fig. 5.14, the critical heat fluxes (CHF) in our experiments range from approximately 28 kW/m^2 to 48 kW/m^2. The CHF in each case is about 10 times larger than the minimum heat flux at the Leidenfrost point. The Leidenfrost point is approached when the inner wall superheat reaches around 50 K. It is evident that the heat flux is decreased to an extremely low value at the Leidenfrost point, because of the inefficient heat transfer mechanism across the vapor layer.

CHAPTER 6

CONCLUSIONS

In the present study, the experiments using liquid nitrogen as coolant have been conducted to understand the effect of the coating layer on cryogenic flow quenching of the stainless steel tubes coated with the Epoxy, Teflon layers and the YSZ layers with different thicknesses were prepared. The surface temperature and heat flux were obtained by measuring the transient central temperatures of the tube and solving the inverse heat conduction equation. The conclusions are drawn as follows

- Epoxy play important role in this study. Epoxy act as a coating material in very pipe. Each low thermal conducting powder materials are coated with epoxy.
- The thin coating layer with low thermal conductivity can shorten the cooling time duration of the quenching process which is attributed to the improvement of the LFP temperature, indicating that the boiling mode changes from film boiling to transition boiling with better heat transfer performance at a higher temperature. The Teflon-coated surface takes less quenching time than the YSZ-coated surface at a similar thickness in the present experiment.
- As comparing Teflon 1 and YSZ 1 coated tubes. YSZ 1 coated tubes takes less quenching time of 315s.
- As comparing Teflon 2 and YSZ 2 coated tubes. Teflon 2 coated tubes takes quenching time of 125s
- The mixture of Teflon and YSZ (the first condition 5.5g Teflon and 4.5g of YSZ, the second condition 6.6 g of Teflon and 5.4 g of YSZ. Both this case the Teflon quantity is more compared to YSZ. So we can concluded as the thickness of Teflon increases the quenching time is shortened.
- The mixing coating layer enables the transition boiling earlier. Consequently the total mass of the LN_2 consumed was reduced by maximum of 64%.

- The enhancement of quenching heat transfer by the coating layer only works within a certain range of thickness. Since the thermal conductivity of the YSZ is larger than that of the Teflon, the cooling time duration of the Teflon -coated surface is shortened moderately with the increasing thickness.

- The critical heat fluxes (CHF) in our experiments range from approximately 28 kW/m^2 to 48 kW/m^2. The maximum heat flux is show by the (Teflon + YSZ) 2 coated surface and is about 48 kW/m^2 and the minimum heat flux is shown by the uncoated surfaces is about 28$kW/m^{2.}$

- The heat transfer coefficient (HTC) in our experiment ranges from 2kW/m^2K to 5kW/m^2K. The maximum heat transfer coefficient is shown by (Teflon + YSZ) 2 coated surface and is about 4.48 kW/m^2K and the minimum heat transfer coefficient is shown by uncoated surfaces and is about 2.42kW/m^2K.

- As the thickness increases the cooling time decreases. Here Teflon is act as a good low conductive layer.

REFERENCES

Burke J C, Byrnes W R, Post A H and Arthur F E R (**1960**) Pressurized cooldown of cryogenic transfer lines. Adv. *Cryog. Eng*. 45: 283–290

Darr S, Hu H, Schaeffer R, Chung J, Hartwig J, Majumdar (**2015**) A. Numerical simulation of the liquid nitrogen chilldown of a vertical tube. *In: SciTech conference, Orlando, FL*.

Darr S R, Hu H and Glikin N G (**2016**) An experimental study on terrestrial cryogenic transfer line chilldown I. Effect of mass flux, equilibrium quality, and inlet subcooling. *Int.J. Heat Mass Transf*. 103: 1225–1242

Daisuke Takeda, Katsuyoshi Fukiba, Hiroaki Kobayashi. (**2017**) Improvement in pipe chilldown process using low thermal conductive layer. *Heat and mass transfer*.2017.03.114

Goswami T K (2010) Role of cryogenics in food processing and preservation. *Int. J. Food Eng*. 6: 2

Gaurav Kumar Singh, Subrata Pradhan, Vipul Tanna (**2019**) Experimental studies of two phase flow characteristics and void fraction predictions in two steady state horizontal two-phase nitrogen flow. Cryogenics 100 (2019) 77-84

Hartwig J, Hu H, Styborski J and Chung J N (**2015**) Comparison of cryogenic flow boiling in liquid nitrogen and liquid hydrogen chilldown experiments. *Int. J. Heat Mass Transf*. 88: 662–673

H. Kim, G. DeWitt, T. McKrell, J. Buongiorno, L.W. Hu, (2009) On the quenching of steel and zircaloy spheres in water-based nanofluids with alumina, silica and diamond nanoparticles, Int. J. Multiphase Flow 35 (5) (2009) 427–438.

Hartwig J, Darr S and Asencio A (**2016**) Assessment of existing two phase heat transfer coefficient and critical heat flux correlations for cryogenic flow boiling in pipe quenching experiments. *Int. J. Heat Mass Transf*. 93:441–463

Hu H, Chung J N and Amber S H (**2012**) An experimental study on flow patterns and heat transfer characteristics during cryogenic chilldown in a vertical pipe. *Cryogenics* 52:268–277

Jackson J, Liao J, Klausner J F and Mei R **(2005**) Transient heat transfer during cryogenic chilldown. *Heat Transfer* 2:253–260

Johnson J and Shine S R (**2015**) Transient cryogenic chilldown process in horizontal and inclined pipes. *Cryogenics* 71: 7–17

Luca Andena and Marta Rink (**2004**) Simulation of PTFE Sintering: Thermal Stresses and Deformation Behavior. *Polymer Engineering and Science*, vol. 44, no. 7

Lingxue Jin, Changgi Park, Hyokjin Cho, Cheonkyu Lee, Sangkwon Jeong. (**2016**) Experimental investigation on chill-down process of cryogenic flow line. *Cryogenics.*2016.08.006

Mohammed J, Mohizin A and Roy K (**2020**) Experimental investigations on transient cryogenic chilldown of a short horizontal copper transfer line. *Sadhana*, 45:12

Shaeffer R, Hu H, Chung JN. (**2013**) An experimental study on liquid nitrogen pipe chilldown and heat transfer with pulse flows. *Int. J Heat Mass Transf* 2013;67: 955–66.

Srinivasan K, Seshagiri Rao V and Krishna Murthy M V (**1974**) Analytical and experimental investigation on cooldown of short cryogenic transfer lines. *Cryogenics* 14:489–494

Sutton GP, Biblarz O.(**2010**) Rocket Propulsion Elements. *eighth edition. Hoboken, NJ: Biblarz John Wiley and Sons*; 2010.

Takeo Tojo, Tooru Atake, Toshiyuki Mori, Hiroshi Yamamura, (**1999**) Heat capacity and thermodynamic functions of zirconia and yttria-stabilized zirconia, *J. Chem. Thermodyn*. 31 (7) 831–845.

V.V. Yagov, M.A. Lexin, A.R. Zabirov, O.N. Kaban'kov, (**2016**) Film boiling of subcooled liquids. Part I: Leidenfrost phenomenon and experimental results for subcooled water, *International Journal of Heat and Mass Transfer*, 100 908-917.

V.V. Yagov, M.A. Lexin, A.R. Zabirov, O.N. Kaban'kov,(**2016**) Film boiling of subcooled liquids. Part I: Leidenfrost phenomenon and experimental results for subcooled water, *International Journal of Heat and Mass Transfer*, 100 908-917.

Weitai Xu, Cheng Cheng, Xudong Song, Peng Zhang.(**2021**) Experimental investigation of cryogenic flow quenching of horizontal stainless steel tube .*cryogenic*s 117(2021) 103327

Yuan K, Ji Y and Chung J N (**2007**) Cryogenic chilldown process under low flow rates. *Int. J. Heat Mass Transf*. 50:4011–4022

Yuan K, Ji Y and Chung J N (**2009**) Numerical modelling of cryogenic chilldown process in terrestrial gravity and microgravity. *Int. J. Heat Fluid Flow* 30: 44–53

Xu W, Zhang P. (*2020*) Cryogenic quenching of a stainless steel rodlet with various coatings. *Int. J Heat Mass Transfer* 2020; 154:119642.